

Diplomarbeit

**Right ventricular function as predictor of outcome after
transcatheter aortic valve implantation (TAVI)**

eingereicht von

Claus Kamml

zur Erlangung des akademischen Grades

Doktor der gesamten Heilkunde

(Dr. med. univ.)

an der

Medizinischen Universität Graz

ausgeführt an der

Universitätsklinik für Innere Medizin, klinische Abteilung für Kardiologie und

Universitätsklinik für Radiologie

unter der Anleitung von

Dr.med.univ.Dr.scient.med. Johannes Schmid

Assoz. Prof. Priv.-Doz. Dr.med.univ.Dr.scient.med. Peter Rainer

Eidesstattliche Erklärung

Ich erkläre ehrenwörtlich, dass ich die vorliegende Arbeit selbstständig und ohne fremde Hilfe verfasst habe, andere als die angegebenen Quellen nicht verwendet habe und die den benutzten Quellen wörtlich oder inhaltlich entnommenen Stellen als solche kenntlich gemacht habe.

Graz, am 26.08.2021

Claus Kamml, eh.

Acknowledgements

First of all, I would like to thank my academic advisors, Dr. Johannes Schmid and Prof. Dr. Peter Rainer, for their guidance. It was a cooperation at eye level throughout the entire work, which does not go without saying and I appreciated that very much. I would also like to thank them for the fact that it was possible to complete most of the work remotely, which was of great importance to me.

The biggest thanks go to my wife Vera without whom I would not be where I am today.

And finally, I would like to thank my parents for their support and guidance throughout my life and during my studies.

Table of contents

Acknowledgements	ii
Table of contents	iii
Glossary and Abbreviations	v
List of Figures.....	vii
List of Tables.....	viii
Zusammenfassung	9
Abstract.....	11
1 Introduction	12
1.1 Aortic Stenosis.....	12
1.1.1 Epidemiology and Aetiology.....	12
1.1.2 Pathophysiology	13
1.1.3 Diagnosis	14
1.1.4 Classification	17
1.1.5 Treatment.....	18
1.2 Risk assessment before aortic valve replacement.....	21
1.3 Assessment of systolic ventricular function	22
1.3.1 Standard parameters	22
1.3.2 Deformation imaging and myocardial strain	22
1.4 Cardiac Magnetic Resonance Imaging.....	25
1.4.1 CMR sequences for aortic stenosis evaluation.....	26
1.4.2 Post processing of CMR deformation imaging	27
1.5 Study aim.....	28
2 Methods	29
2.1 Study Design	29
2.2 Study Population	29
2.2.1 Inclusion criteria.....	29
2.2.2 Exclusion criteria.....	29
2.3 Data Collection.....	29
2.3.1 Clinical data.....	29
2.3.2 Cardiac Magnetic Resonance Imaging.....	30
2.3.3 Volumetric analysis	30
2.3.4 Strain analysis.....	31
2.4 Statistical Analysis	32

3	Results	33
3.1	Baseline characteristics of study population	33
3.2	Descriptive statistics of CMR parameters of volumetry and deformation imaging	40
3.3	Interventricular correlations of CMR parameters, Laboratory parameters and haemodynamic parameters	41
3.4	Survival Analysis.....	43
3.5	Interventricular Interactions	48
3.6	Interobserver Reliability	49
4	Discussion.....	49
4.1	Limitations.....	51
4.2	Conclusion and Outlook	52
5	References	53

Glossary and Abbreviations

AS	Aortic stenosis
AVA	Aortic valve area
CABG	Coronary artery bypass graft
CK	Creatine kinase
CKMB	Creatine kinase Myocardial Band
CMR	Cardiac magnetic resonance imaging
CO	Cardiac output
CPC-PH	Combined pre- and post-capillary pulmonary hypertension
CV	Coefficient of variation
ECG	Electrocardiogram
ED	End-diastole
EDV	End diastolic volume
EDVI	End diastolic volume index
EF	Ejection fraction
ES	End-systole
ESC	European society of cardiology
GCS	Peak global circumferential strain
GLS	Peak global longitudinal strain
HR	Hazard ratio
hs-TrT	Troponin T high sensitive
LAX	Long axis
LV	Left ventricle
LV-MMI	Left ventricular myocardial mass index
NT-proBNP	N-terminal pro-B-type natriuretic peptide
PAD	Peripheral arterial disease
PVR	Pulmonary vascular resistance
RV	Right ventricle
SAVR	Surgical aortic valve replacement
SAX	Short axis
STS-Score	Society of thoracic surgeons risk model
SV	Stroke volume
SVI	Stroke volume index

TAPSE	Tricuspid annular plane systolic excursion
TAVI	Transcatheter aortic valve implantation
TDI-E/e'	Tissue doppler imaging ratio between early mitral inflow velocity and mitral annular early diastolic velocity
TEE	Transesophageal echocardiography

List of Figures

Figure 1: Structural and functional changes and hemodynamics of severe aortic stenosis.	14
Figure 2: Average course of aortic stenosis	19
Figure 3: Myocardial strain and strain rate curves.	24
Figure 4: Schematic representation of the spatial directions of myocardial deformation. ..	24
Figure 5: Short axis stack of images using SSFP cine CMR.	27
Figure 6: 3D model of the heart generated via tissue tracking.....	28
Figure 7: End-diastolic SAX slice with outlines of endo- and epicardial contours.	31
Figure 8: LAX-4-chambers slice of the heart in the tissue tracking module.....	32
Figure 9: Flow chart of study population after exclusion.....	35
Figure 10: Histograms of baseline characteristics and standard parameters.	37
Figure 11: Gender distribution of patients.....	40
Figure 12: Scatterplots of correlations between RV- pulmonary- and hemodynamic- parameters.....	41
Figure 13: Kaplan-Meier survival curve in RV-GLS groups divided by Youden Index. ...	45
Figure 14: Kaplan-Meier survival curve in RV-EDVI groups divided by Youden Index. .	45
Figure 15: Kaplan-Meier survival curve in RV-EF groups divided by Youden Index.	46

List of Tables

Table 1: Strengths and weaknesses of standard CMR sequences (27,29).....	26
Table 2: Baseline characteristics of study population.	36
Table 3: Characteristics of CMR derived parameters of volumetry and deformation.	40
Table 4: Pearson correlations between RV parameters and pulmonary hemodynamic, LV and laboratory parameters of heart failure.....	41
Table 5: Univariate Cox Regression prediction of cardiovascular mortality after 1-, 2- and 3-years.	44
Table 6: Univariate cox-regression for dichotomized RV-parameters for 1-, 2- and 3-year cardiovascular mortality.	45
Table 7: RV-parameters and age in multivariate Cox regression for 3-year cardiovascular mortality.	46
Table 8: RV-parameters and sex in multivariate Cox regression for 3-year cardiovascular mortality.	46
Table 9: RV-parameters and NT-proBNP in multivariate Cox regression for 3-year cardiovascular mortality.	47
Table 10: RV-parameters and STS-Score in multivariate Cox regression for 3-year cardiovascular mortality.	47
Table 11: RV parameters and LV-EF in multivariate Cox regression for 3-year cardiovascular mortality.	47
Table 12: Multivariate cox regression for cardiovascular mortality with model containing LV-EF and LV-MMI.	48
Table 13: RV parameters and MPAP in multivariate Cox regression for 3-year cardiovascular mortality.	48
Table 14: RV parameters and PCWP in multivariate Cox regression for 3-year cardiovascular mortality.	49
Table 15: Interobserver Reliability.....	49

Zusammenfassung

Einleitung: Die Aortenstenose (AS) ist die häufigste primäre Herzklappenerkrankung in Europa und Nordamerika und mit einer erheblichen Morbidität und Mortalität verbunden. Die einzige Behandlung, die nachweislich das Überleben bei schwerer AS verbessert, ist der Klappenersatz. In der derzeitigen klinischen Praxis wird die Entscheidung zwischen einer Transkatheter-Aortenklappenimplantation (TAVI) und einem chirurgischen Aortenklappenersatz von einem interdisziplinären Team auf der Grundlage kardialer und extrakardialer Merkmale von Patientinnen und Patienten sowie verschiedener Risikoscores getroffen. Neuere Studien haben gezeigt, dass keiner der etablierten Risikoscores eine zufriedenstellende Risikovorhersage bei Patientinnen und Patienten, die sich einer TAVI unterziehen, erreichen konnte. Es gibt zunehmend Hinweise, dass rechtsventrikuläre Parameter die Mortalität bei Patientinnen und Patienten, die sich einer TAVI unterziehen, vorhersagen.

In dieser Studie soll untersucht werden, ob rechtsventrikuläre Parameter, die mittels kardialer Magnetresonanztomographie (CMR) gewonnen werden, die Mortalität bei Patientinnen und Patienten, die sich einer TAVI unterziehen, vorhersagen können und einen zusätzlichen Wert für die Risikobewertung haben könnten.

Methoden: Patientinnen und Patienten mit schwerer Aortenstenose wurden prospektiv rekrutiert, um sich vor einer TAVI einer 1.5T-CMR zu unterziehen. Nach Ausschluss von 11 Patientinnen und Patienten wurden die CMR-Bilder von 112 Patientinnen und Patienten mittels Tissue-Tracking-Software (Circle cvi42) analysiert. Zu den gewonnenen Parametern gehörten volumetrische Daten wie Ejektionsfraktion (EF) und enddiastolischer Volumen Index (EDVI), sowie die Parameter der Wandbewegungsanalysen wie globaler longitudinaler und zirkumferenzieller Strain (GLS, GCS) von linkem und rechtem Ventrikel (LV, RV). Diese Parameter wurden mit Baseline-Charakteristika, invasiv gemessenen hämodynamischen Parametern und Labormarkern korreliert und Assoziationen mit dem Outcome mittels uni- und multivariater Cox-Regression analysiert. Primärer Endpunkt war die 3-Jahres kardiovaskuläre Mortalität, sekundäre Endpunkte waren die 2-Jahres und 1-Jahres kardiovaskuläre Mortalität.

Ergebnisse: Die mittlere Nachbeobachtungszeit betrug 3.9 Jahre (2.3-2.7). Die Mortalität nach 1 und 3 Jahren betrug 14.3% (16/112) bzw. 28.6% (32/112). Die durchschnittliche mittels CMR erhobene RV-EF war $54.6 \pm 12.8\%$, der durchschnittliche RV-GLS war $-21.3 \pm 5.8\%$, der durchschnittliche RV-GCS war $-13.5 \pm 3.6\%$, die mediane RV-EDVI war 74.6ml (IQR 63.2 -92.2). RV-EF, RV-GLS und RV-EDVI waren in der univariaten Cox-

Regression signifikante Prädiktoren für die 3-Jahres kardiovaskuläre Mortalität. LV-EF und LV-GCS sagten weder die Ein-, Zwei- noch die Drei-Jahres kardiovaskuläre Mortalität voraus. In der multivariaten Cox-Regression zeigte sich, dass RV-EF und RV-EDVI signifikante Prädiktoren für die kardiovaskuläre Mortalität nach drei Jahren blieben, wenn sie für Geschlecht und Alter adjustiert wurden, während RV-GLS nur für das Geschlecht signifikant blieb.

Fazit: CMR-abgeleitete RV-Funktionsparameter zeigten in unserer Kohorte einen guten prädiktiven Wert für die ein-, zwei- und drei Jahres kardiovaskuläre Mortalität. Sie schnitten besser ab als linksventrikuläre Funktionsparameter und könnten die Vorhersage des Outcomes nach TAVI verbessern. Weitere Studien sind erforderlich, um eine mögliche Integration von rechtsventrikulären Parametern in bestehende Risiko-Scores zu evaluieren.

Abstract

Introduction. Aortic Stenosis (AS) is the most prevalent primary valvular heart disease in Europe and North America and associated with considerable morbidity and mortality. The only treatment shown to improve survival in severe AS is valve replacement. In current clinical practice the decision between transcatheter aortic valve implantation (TAVI) and surgical aortic valve replacement is made by an interdisciplinary team based on cardiac and extracardiac characteristics of the patient as well as several risk scores. Recent studies have shown that none of the established risk scores were able to achieve a satisfactory level of risk prediction in patients undergoing TAVI. There is growing evidence that right ventricular (RV) parameters predict mortality in patients undergoing TAVI.

This study seeks to determine if RV parameters obtained via cardiac magnetic resonance imaging (CMR) can predict mortality in patients undergoing TAVI and might be of additional value in preprocedural risk evaluation.

Methods. Patients with severe AS were prospectively recruited to undergo 1.5T-CMR before TAVI. After exclusion of 11 patients, CMR images of 112 patients were analysed using dedicated tissue tracking software (Circle cvi42). Obtained parameters included volumetric data, such as ejection fraction (EF) and end-diastolic volume index (EDVI), and global longitudinal and circumferential myocardial strain (GLS, GCS) of both the left ventricle (LV) and RV. These parameters were correlated with clinical data including invasively measured haemodynamic parameters and laboratory markers and were associated with outcomes in uni- and multivariate cox regressions. Primary endpoint was 3-year cardiovascular mortality, secondary endpoints were two-year and one-year cardiovascular mortality.

Results. Median follow-up was 3.9 years (2.3-2.7). Mortality after one and three years was 14.3% (16/112) and 28.6% (32/112), respectively. Mean CMR derived RV-EF was $54.6 \pm 12.8\%$, mean RV-GLS was $-21.3 \pm 5.8\%$, mean RV-GCS was $-13.5 \pm 3.6\%$, median RV-EDVI was 74.6ml (IQR 63.2 -92.2). RV-EF, RV-GLS and RV-EDVI were significant predictors of three-year cardiovascular mortality in univariate Cox regression, while LV-EF and LV-GCS did not predict cardiovascular mortality. In multivariate cox regression we found that RV-EF and RV-EDVI remained significant predictors for cardiovascular mortality after three years when adjusted for sex and age, whereas RV-GLS remained significant for sex.

Conclusion. CMR derived RV functional parameters showed good predictive value for one-, two- and three-year cardiovascular mortality in our cohort. They performed better

than LV functional parameters and may improve prediction of outcome after TAVI. Further studies are needed to evaluate a possible integration of RV parameters into existing risk scores.

1 Introduction

Aortic stenosis (AS) is the most prevalent primary valvular heart disease in Europe and North America and associated with considerable morbidity and mortality. The only treatment shown to improve survival in AS is valve replacement. In current clinical practice the decision between trans aortic valve implantation (TAVI) and surgical aortic valve replacement (SAVR) is made by an interdisciplinary team based on cardiac and extracardiac characteristics of the patient as well as several available risk scores including Euro Score II, German AV Score and STS score. Recent studies have shown that none of the established risk scores were able to achieve a satisfactory level of risk prediction in patients undergoing TAVI (1–3). None of the mentioned risk scores implement right ventricular (RV) parameters, even though studies have shown strong predictive value (4,5). This study seeks to determine the prognostic value of cine cardiac magnetic resonance imaging (CMR) derived RV parameters such as RV global circumferential strain (RV-GCS), RV global longitudinal strain (RV-GLS), RV ejection fraction (RV-EF) and other functional parameters obtained via CMR regarding cardiovascular mortality.

1.1 Aortic Stenosis

AS is defined as a congenital or acquired disorder of the aortic valve that causes insufficient opening of the valve (6). In the following chapter, all relevant aspects of aortic stenosis from epidemiology and aetiology to diagnostics and therapy are discussed, for they are fundamental to this thesis.

1.1.1 Epidemiology and Aetiology

Today, AS is the third most common cardiovascular disease. Due to demographical changes in the population the prevalence is constantly rising making aortic valve replacement the most frequently performed valve replacement in Europe. At 65 years of age the frequency of aortic valve sclerosis is approximately 25% rising to 48% at 75 years (7).

The most common cause of AS is degenerative calcification of a tricuspid valve. This pathogenesis accounts for 80% of cases in Western countries and is characterised by a

progressive calcification progressing from the base of the cusps to the commissures. The second most common cause of AS is endocarditis due to rheumatic disease, which has been the leading cause for AS in the past but has markedly declined in prevalence since the widespread use of antibiotics in the treatment of streptococci infections (8). Congenital bicuspid aortic valves are associated with a higher risk for AS and account for most cases in the population younger than 60 years. This trend is reversed at a higher age where the normal anatomical variant is most commonly seen. Other rare causes are familial hypercholesterolaemia, hyperuricaemia, hyperparathyroidism, Paget disease, ochronosis, Fabry disease, lupus erythematosus, and drug-induced diseases (7).

1.1.2 Pathophysiology

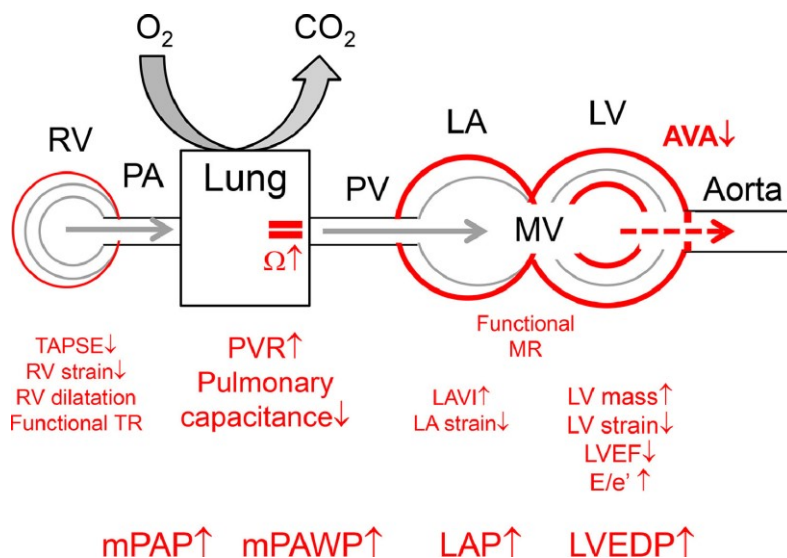
The pathophysiology of AS is an active process including chronic inflammation, lipoprotein deposition, renin–angiotensin system activation, osteoblastic transformation of valvular interstitial cells, and active calcification. This process is very similar to atherosclerosis and associated with well-established cardiovascular risk factors such as hypertension, smoking, diabetes, elevated cholesterol levels making it an atherosclerosis-like process. New findings however suggest that the pathogenesis of AS might be more intricate and suggest that there are specific cell-signalling pathways regulating valvular calcification such as BMP2/RANK/runx2/Cbfa1. Familial clusters and recent findings implicating genetic polymorphisms of the vitamin D receptor and mutations such as in the NOTCH1 gene in bicuspid aortic valves suggest that genetic factors may also influence valve pathogenesis (7).

Typically, the severity of AS is described using the transvalvular gradient and valve opening area. However, it has recently been recognized that this does not adequately describe the severity of the disease in its entire extent. More recent approaches have focused on the stage of damage to the myocardium, pulmonary vasculature, and consequently, the right heart. This approach may also provide a better prediction of survival, as the key factor for long-term survival is the reversibility of the remodelling resulting from AS (9,10).

If left untreated, the increased pressure on the LV caused by the stenosis initially leads to compensation by means of myocardial hypertrophy. The increase in wall thickness compensates for the increased pressure while the wall strain remains constant. In the course of the disease, however, the hypertrophy is followed by fibrosis and, as a result, reduced relaxation, and increased stiffness. Consequently, there is increased end-diastolic

pressure in the ventricle and later in the atrium. In addition, there is an increasing decrease in myocardial strain with initially preserved LV-EF and eventually a decrease in LV-EF as well. In the course, mitral regurgitation and left atrial dysfunction can lead to pulmonary hypertension of a post capillary type. Chronic pulmonary hypertension, in turn, leads to vascular remodelling, which is not yet fully understood in patients suffering from AS. However, there is new evidence for patients suffering from heart failure with preserved EF, demonstrating global pulmonary vascular remodelling that is associated with worse outcome. Fayyaz et al. found that the severity of PH correlates with intima thickening in venous and small intermediate vessels (11). Hemodynamically, these changes are best reflected by pulmonary vascular resistance (PVR) or the combination of pre- and post-capillary pulmonary hypertension (CPC-PH)(9). A depiction of the interventricular interaction is presented in **Figure 1**.

Figure 1: Structural and functional changes and hemodynamics of severe aortic stenosis.



LAP=left atrium pressure, LVEDP=left end diastolic pressure, PA=pulmonary artery; Reproduced from (9) under the Creative Commons CC-BY-NC-ND license.

1.1.3 Diagnosis

1.1.3.1 Symptoms

AS is typically asymptomatic in the early stages of the disease, making an early diagnosis usually the result of chance findings. Even with severe AS 50% of patients remain asymptomatic for many years. Unfortunately, prognosis in symptomatic patients decreases

significantly with a two-year survival after onset of symptoms of 50%, making an early diagnosis key for an effective treatment.

Patients suffering from AS may present with chest pain and tightness, arrhythmia, dizziness and fainting during activity. When untreated, symptoms progress, leading to heart failure with shortness of breath and oedema (9).

Since patients with increasing aortic valve stenosis may limit their activities during the course of the disease can lead to masking of the severity, it is necessary to correctly classify patients into symptomatic and non-symptomatic groups by extended diagnostics such as stress testing. Additionally, findings like ST-segment depression, ventricular arrhythmias, and inadequate rise of systolic blood pressure during treadmill testing are indicators of poor prognosis and have a class I recommendation for aortic valve replacement (10).

1.1.3.2 Clinical examination and auscultation

In the physical examination a slow rising carotid pulse due to a prolonged LV ejection can be seen and a reduction in stroke volume (SV) can lead to a small amplitude pulse. The most specific finding is a crescendo-decrescendo murmur evident over the second intercostal space on the right side of the sternum in auscultation, which is transmitted to the carotids. The intensity of the murmur is suggestive of the severity but may be hard to interpret because of obesity, underlying pulmonary disease or reduced cardiac output (CO).

1.1.3.3 Echocardiography

Echocardiography is the gold standard in the diagnosis of AS to date. In addition to the evaluation of the aortic valve, it provides information on LV function and other valves. In principle, signs of AS can be detected in 2-dimensional echocardiography alone, that can show thickened and calcified aortic valve leaflets with reduced leaflet motion. However, to determine the degree of severity doppler echocardiography is essential. Continuous wave doppler spectra, that in contrast to pulsed wave doppler allow measurements of high velocities, are acquired from the aortic valve. From these spectra, peak and mean systolic velocities can be measured and allow the calculation of gradients via the simplified Bernoulli equation. In severe cases of AS, high systolic flow can be detected that in general correlates well with stenosis severity. However, in some cases a low pressure-gradient due to limited LV function can mask the severity of the stenosis. Therefore, a low pressure-gradient does not exclude a significant stenosis and calculation of the aortic opening area with the continuity equation is mandatory. The continuity equation requires

additional measurements of the LVOT diameter from a parasternal long axis view and systolic velocities in the LVOT via pulsed wave doppler. An aortic opening area smaller than 1 cm² or 0.6 cm²/m² when indexed to the body surface area indicates severe AS (12).

1.1.3.4 Electrocardiography

In the electrocardiogram (ECG) LV hypertrophy can be observed, however is neither specific nor sensitive to the prevalence of AS. In later stages of the disease, a left bundle branch block or a complete AV block might be evident in case the degeneration of the aortic valve impairs the excitation conduction system. These ECG findings are however not specific of AS and are regularly seen in other heart diseases.

1.1.3.5 Stress-Electrocardiography

While in the past, exercise testing was not recommended in all patients with AS, consensus today is that it should not be performed in patients with symptomatic AS. However, in supposedly asymptomatic patients it is acceptable and may reveal limited exercise tolerance or even stress-related symptoms. Due to pre-existing ECG changes and limited coronary flow reserve, the information about the presence of coronary artery disease is limited. A stress-induced drop in blood pressure indicates an unfavourable course and is a sufficient indication for an aortic valve replacement.

Low-dose dobutamine stress can be utilised to distinguish between severe AS and pseudosevere AS (low flow low gradient AS with modest flow reserve) by calculating the projected aortic valve area. In the case of pseudosevere AS there is a persistent discordance between AVA and mean gradient (i.e. AVA remains <1 cm², mean gradient remains <40 mmHg) (13).

$$\textit{Projected AVA} = \textit{AVARest} + [(\textit{AVAPeak} - \textit{AVARest})/(\textit{QPeak} - \textit{QRest})] \times (\textit{250} - \textit{QRest})$$

Q = mean transvalvular flow rate = (stroke volume)/(LV ejection time)

Although a submaximal stress test under medical supervision is considered harmless, patients with moderate or severe AS should not expose themselves to excessive physical stress in their daily lives (12).

1.1.3.6 Chest X-Ray

The heart size on X-ray is usually normal, since myocardial hypertrophy is often concentric, meaning that wall thickening is at the expense of the cavity. The aortic arch is prominently displayed in case of post stenotic dilatation. On the lateral images, calcified aortic valve leaflets can often be seen in degenerative aortic valve stenosis.(12)

1.1.3.7 Multi-detector computed tomography

Multi-detector computed tomography (MDCT) is the diagnostic modality of choice to separate patients suffering from pseudo severe AS, that typically do not benefit from TAVI, from patients with true severe AS. Patients with no significant increase in flow rate (<15%) during dobutamine stress echocardiography (DSE) are particularly difficult to classify via DSE alone and should be examined by MDCT to determine the amount of calcification in the AV. Using the aortic valve calcification score, it is possible to classify severe and pseudo-severe AS based on cut-off values (13).

1.1.4 Classification

The classification of AS is determined by assessment of data obtained via Doppler Echocardiography. The relevant parameters in clinical practice today are valve opening area, mean pressure gradient, EF and stroke volume index (SVi)(14).

- **High-gradient AS** (valve area <1 cm², mean gradient >40mmHg). In this case severe AS is evident regardless of LV-EF.

- **Low-flow, low-gradient AS with reduced ejection**

fraction (valve area <1 cm², mean gradient <40mmHg, ejection fraction <50%, SVi ≤35mL/m²).

- **Low-flow, low-gradient AS with preserved ejection**

fraction (valve area <1 cm², mean gradient <40mmHg, ejection fraction ≥50%, SVi ≤35mL/m²). Typical finding in the elderly, associated with LV hypertrophy and a history of hypertension as well as small ventricle size. Diagnosis of this form of AS is demanding

and needs careful exclusion of other causes or measurement errors. The presence and degree of valve calcification determined by Multislice-CT is associated with severity and outcome and therefore increasingly relevant in this setting.

- **Normal-flow, low-gradient AS with preserved ejection**

fraction (valve area $<1 \text{ cm}^2$, mean gradient $<40\text{mmHg}$, ejection fraction $>50\%$, SVi $>35\text{mL/m}^2$). These patients may suffer from moderate AS but a careful consideration of other factors like further diagnostic findings, symptoms and laboratory values (i.e. NT-proBNP) is needed to identify cases of severe AS presenting with the above mentioned findings in echocardiography.

1.1.5 Treatment

1.1.5.1 Medical Treatment

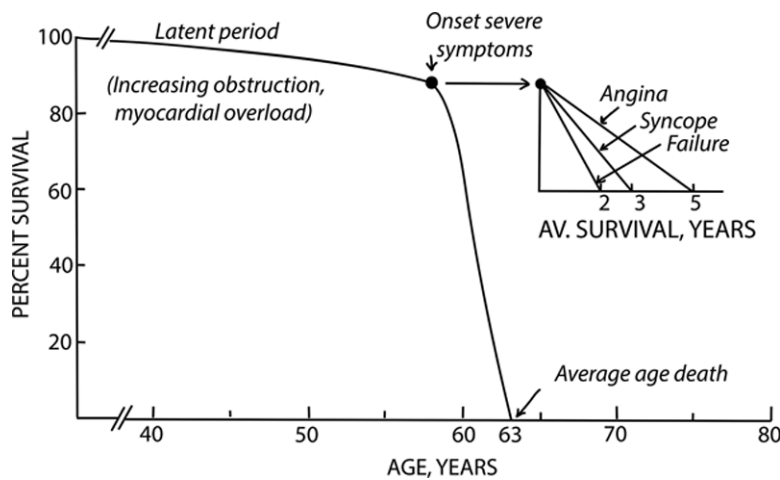
The treatment of AS depends not only on the type of stenosis but also on the patient's individual risk profile and age. The presence of symptoms is crucial for the initial need for intervention because the prognosis worsens significantly after symptoms appear, as shown in **Figure 2**.

After diagnosis, the appropriate intervention strategy is selected based on the classification and personal risk profile.

To date no pharmaceutical therapy has shown significant improvement of survival or progression of AS (7,10,11). Current European Society of Cardiology (ESC) guidelines for AS suggest following the established guidelines for heart failure treatment to manage symptoms. These include digoxin, diuretics, angiotensin-converting enzyme inhibitors, or angiotensin receptor blockers if they experience symptoms of heart failure. It is important to note though, that all afterload reducing medication must be used with care for they may cause reduced perfusion of the coronary arteries.

Even though there is no effective medical treatment today, there is a lot of research focusing on cardiovascular risk factors. Due to the pathophysiology of AS, statins are an obvious object of research, but so far no randomized study could prove their effectiveness in AS (7,15). Management of cardiovascular risk factors however is advisable to avoid the progression of comorbidities.

Figure 2: Average course of aortic stenosis



Reproduced from (16) with permission of the publisher. Copyright © 1968, American Heart Association.

1.1.5.2 Surgical aortic valve replacement

SAVR has long been the gold standard for the treatment of symptomatic AS and has been performed for more than 50 years. This procedure is performed on full cardiopulmonary bypass. Typically, a median sternotomy is performed, and the diseased aortic valve is removed completely.

Newer techniques, so called minimally invasive surgical aortic valve replacement, involve smaller chest incisions as opposed to full sternotomy. The two main techniques are mini-sternotomy and mini-thoracotomy.

Multiple meta-analyses found TAVI and SAVR to be similar in terms of mortality however with a different set of complications. In SAVR the most common complications are Major bleeding, new-onset atrial fibrillation, stroke, repeated hospitalization and vascular complications (17).

1.1.5.3 Transcatheter aortic valve implantation

1.1.5.3.1 Indication for Intervention

Due to the unfavourable prognosis of untreated, symptomatic AS, early intervention is important. Patients at high age and comorbidities as well as patients with severe comorbidities leading to a life expectancy of less than 1 year are not recommended for TAVI. The interventional risk outweighs the possible benefit in these cohorts (14,18).

Indication for intervention in asymptomatic AS is controversial. In the current ESC guideline, TAVI is not recommended in asymptomatic patients, even if AS is severe.

Intervention may be considered for patients who develop symptoms in exercise testing or

are likely to develop symptoms in the near future. In these cases, a careful risk-benefit analysis is required (7,14).

1.1.5.3.2 Patient selection for TAVI

The decision which patients are best suitable for TAVI or SAVR is made by a multi-professional team. The so-called Heart Team discusses each case in detail and makes its decision taking into account cardiac and extracardiac characteristics, individual risk, local experience and outcome data (14,18).

Typically, TAVI is recommended for elderly patients with high interventional risk. SAVR, however, is preferred in younger patients with less interventional risk, asymptomatic AS or patients with cardiovascular disease who undergo coronary artery bypass graft (CABG). Recent guidelines do not generally recommend TAVI for low or intermediate risk patients however recognise that there is growing evidence for the safe and effective use in these groups (18–22).

1.1.5.3.3 TAVI access sites

Femoral access

The most common access in the majority of TAVI procedures is the femoral artery. The benefits are a fully percutaneous approach under local anaesthesia and sedation, minimizing the risks involved in general anaesthesia.

Although the technical aspect of the femoral approach is simple, it must be preceded by a detailed diagnostic procedure to evaluate the suitability of the individual anatomical situation. Unprepared femoral approach can lead to serious vascular complications and must be avoided (23).

The gold standard for pre-procedural assessment is CT-angiography, providing information of all possible access sites. In the femoral approach, the iliac and femoral vessels are evaluated with special attention to their diameter, which should not be less than 5.5mm, ideally more than 6.5mm to allow the use of a 16F delivery system. Atherosclerotic plaques, calcification and tortuosity may be contraindications.

Besides the iliac and femoral arteries, the aortic root and arch must be screened for aneurysms, tortuosity, thrombotic appositions or calcification. These findings may cause embolization, vascular rupture or dissection(23).

Trans-axillary/trans-subclavian access

If the femoral approach is contraindicated, the trans-axillary approach is considered the second choice in most centres. The right subclavian artery is chosen as the access site only

in exceptional cases, since there is an unfavourable angle to the aortic annulus. The most commonly used and far more feasible route is via the left axillary artery, which is the continuation of the left subclavian artery. Access site is the proximal third of the axillary artery between the lateral edge of the first rib and the medial border of the pectoralis minor muscle (23).

Direct transaortic access

Another access site is the direct transaortic access via mini-thoracotomy or mini-sternotomy. The ascending aorta is first exposed and then punctured with a guidewire to position the prosthetic valve within the native aortic valve. It is performed under general anaesthesia and intubation. This method is a feasible alternative to the trans-apical approach with similar success rates but without the risk of apical scarring, apical aneurysms, late arrhythmias or ventricular rupture. Contraindications are the presence of thorax deformities, short ascending aorta, porcelain aorta and the presence of a venous coronary artery bypass graft (23).

Transapical access

This approach is the historic primary alternative to the femoral approach and is performed under general anaesthesia via left mini-thoracotomy. The apex of the heart is exposed and punctured to gain direct access through the LV to the aortic annulus. The valve prosthesis is then positioned via a guidewire and expanded.

Contraindications are severely reduced LV-EF and the presence of an apical thrombus. This method is an alternative for patients suffering from severe vascular disease without the possibility for any other approach. 30-day mortality is higher compared with the femoral approach. Whether or not this is due to the unfavourable risk profile of patients or the procedure itself is still being debated (23).

1.2 Risk assessment before aortic valve replacement

Perioperative risk assessment is undertaken by the heart-team with the help of several risk scores as well as clinical and diagnostic characteristics of every individual patient. This step is critical to ensure the optimal means of intervention. According to the current ESC guideline (14) these factors are:

Clinical characteristics: STS score, EuroSCORE II, presence of severe comorbidities (if not reflected by scores), age, frailty, previous cardiac surgery, restricted mobility and suspicion of endocarditis.

Anatomical and technical aspects: Favourable access for TAVI, sequelae of chest radiation, porcelain aorta, presence of intact CABG, possible patient-prosthesis mismatch, severe chest deformity or scoliosis, short distance between valve annulus and coronary ostia, aortic valve annulus size, aortic root morphology and valve morphology.

1.3 Assessment of systolic ventricular function

1.3.1 Standard parameters

Ejection Fraction (EF)

EF is defined as the proportion of SV to total blood volume in the ventricle at the end of diastole, the end-diastolic volume (EDV). Ejection fraction is a measure of cardiac function and is determined by echocardiography, cardiac catheterization, CMR resonance imaging (MRI) or single photon emission computed tomography (SPECT). The reference range is 60-70% in adults at rest (24). Although it is today the most commonly used parameter to classify heart function it has its limitations. Under certain conditions, LV-EF can be normal although LV systolic function is impaired, for it does not directly measure myocardial contractility. Another weakness of EF is, that in case of significant mitral regurgitation it may not reflect the true forward EF. Furthermore, it is highly load-dependent (25).

Tricuspid annular plane systolic excursion (TAPSE)

TAPSE is an echocardiographic parameter for quantification of systolic RV function. For this purpose, M-mode imaging is performed in the apical four-chamber view, in which the axis passes through the lateral annulus fibrosus cordis of the tricuspid valve. In this plane, the motion excursion in systole is measured (24). TAPSE can also be used as a surrogate for longitudinal free wall motion, thus providing an indication of right ventricular function. TAPSE can also be quantified in CMR by measuring the excursion of the tricuspid valve plane between systole and diastole.

1.3.2 Deformation imaging and myocardial strain

Traditionally, cardiac function has been determined using volume-based measurement of EF, visual assessment of local wall motion abnormalities, or change in wall thickness.

These methods are either investigator-dependent and difficult to standardize, or sensitive to loading conditions. This led to a need for more reliable and standardized parameters to objectify measurements and improve reproducibility.

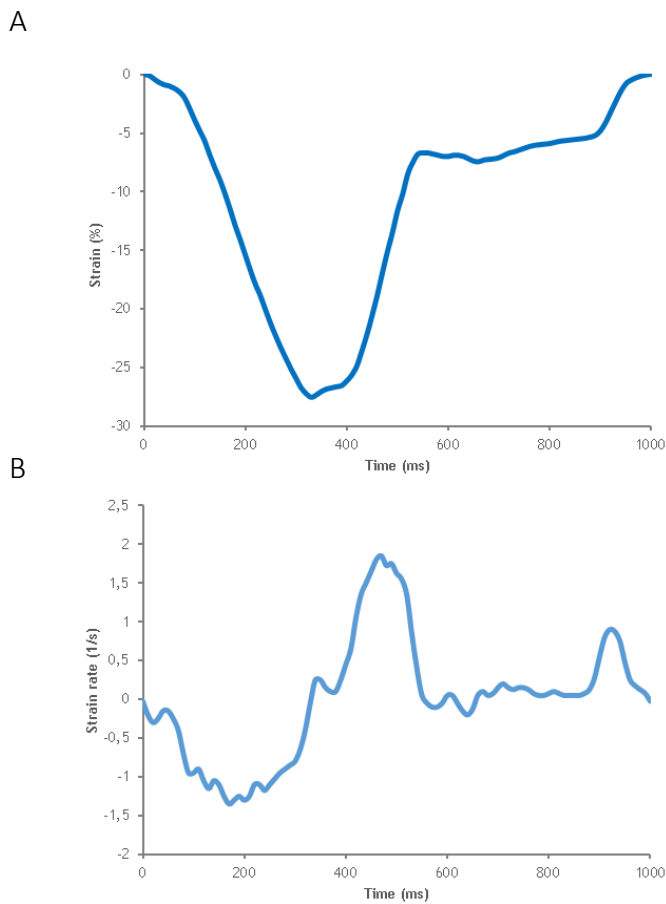
Deformation imaging allows the quantitative assessment of myocardial motion and, consequently, provides less interference-prone parameters to describe regional wall motion and contractility (26).

The technique is based on the detection of myocardium in imaging procedures and a tracking of the movement over time. This allows for an accurate description of the motion and deformation over time and enables direct measurement of muscle shortening and thickening. The fraction of shortening compared to the length in diastole can be expressed as strain in percent (**Figure 4**). The first derivative of the resulting curve represents the strain rate (**Figure 3**).

1.3.2.1 GLS and GCS

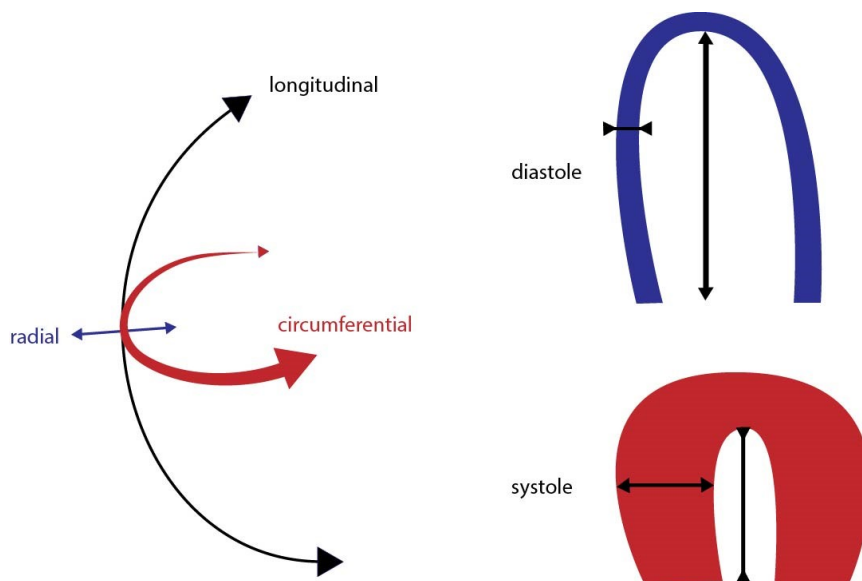
Global longitudinal strain is a measure of global myocardial contractility. It can be measured by two-dimensional (2D) speckle-tracking echocardiography (STE) or feature tracking in CMR. After outlining the myocardium (**Figure 7**) in dedicated software, the myocardium is automatically or semi-automatically tracked and strain is calculated for every myocardial pixel in the image over the entire cardiac cycle. An exemplary strain curve is shown in **Figure 3**. Maximum systolic contraction is represented by peak systolic myocardial strain. This can be done for every slice in CMR. By combining all the layers and calculating the mean global peak strain in a circumferential or longitudinal direction (**Figure 4**), a robust measure of global myocardial contraction is obtained which will be referred to as GCS and GLS in the further course.

Figure 3: Myocardial strain and strain rate curves.



A: Typical myocardial longitudinal strain curve of the left ventricle during one heart cycle. B: Corresponding myocardial strain rate.

Figure 4: Schematic representation of the spatial directions of myocardial deformation.



1.4 Cardiac Magnetic Resonance Imaging

After purely scientific application at the beginning, CMR is now a robust diagnostic option for the evaluation of a range of cardiological entities. Although it has not yet been incorporated into current guidelines for standard evaluation of valve disease, it is the gold standard for non-invasive assessment of LV and RV volumes and EF (27,28).

In addition to precise determination of cardiac volumes, CMR also allows accurate assessment of myocardial thickness, wall motion and ventricular mass (28).

CMR can provide information about a variety of cardiac conditions. The cardiac diseases with the corresponding sequences along with their advantages and disadvantages are summarized in **Table 1**.

Table 1: Strengths and weaknesses of standard CMR sequences (27,29).

Sequence	Purpose	Strengths	Weaknesses
T1 mapping	Myocardial fibrosis	Identify earlier diffuse fibrosis and without the need for local reference.	No consensus in the CMR community's methodology and approach. Lack of histological validation.
T2 weighted imaging (T2W-TSE with dark blood preparation and fat-suppression or STIR (short tau inversion))	Oedema, Infiltration	Detection of myocardial fluid content by longer T2 relaxation time	Low SNR Incomplete blood suppression at endocardial boundary layer. Unreliability due to diastolic cardiac motion ECG mistriggering. Poor breathhold
Stress first-pass myocardial perfusion	Cardiomyopathy related perfusion defects/exclusion of concurrent epicardial coronary artery disease	Higher spatial resolution than SPECT	Incomplete myocardial coverage. "Dark-rim" artefact. Cardiac motion during image
Early Gadolinium enhancement (EGE)	Microvascular obstruction, Detection of intracardiac thrombus	High spatial resolution	Dependent on image timing after injection. ECG mistriggering. Poor breath hold
Late Gadolinium enhancement (LGE)	Myocardial fibrosis	High T1 contrast of diseased myocardium	Image contrast depends on inversion time adjustment and Gad washout. Ghosting from long T1 fluids (can be suppressed). ECG mistriggering. Poor breath-hold.
Breath hold balanced SSFP cine	Global regional myocardial function and wall thickness	High signal to noise ratio (SNR), (T2/T1) image contrast gives reliable blood: myocardium endocardial border definition based on long T2 of blood	Sensitive to field inhomogeneity (off-resonance banding artefact). ECG-mistriggering/ Poor breath hold

Table of different CMR sequences and their diagnostic use along with strengths and weaknesses.

1.4.1 CMR sequences for aortic stenosis evaluation

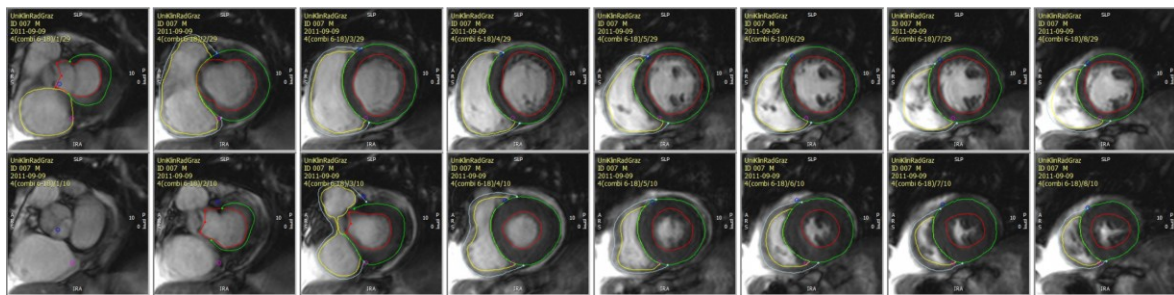
Cine steady-state free precession (SSFP)

SSFP is the most frequently used sequence in clinical practice and provides ECG triggered temporal images representing myocardial movement during one heart cycle by generating a set of sequential images in both short-axis (axial: every 10mm from base to apex) and

long-axis (longitudinal: 1-4 slices of 2-, 3-, and 4-chamber views). With these ultrafast pulse sequences, a temporal resolution of 25 to 35ms can be achieved providing frame rates of 30-40/s (22).

The images are acquired during multiple captures while the patient is instructed to hold his or her breath to minimize artifacts caused by breathing motion. For this method, a 5-6 second breath hold is typically sufficient and tolerable for most patients. These stacks of temporally aligned images allow the tracking of myocardial movement over time in 2 and 3-dimensions via post-processing in specialized software. In addition, it is possible to evaluate the number and motion of aortic valve cusps visually in a slice through the aortic valve plane and calculate the aortic valve area (AVA) via planimetry (28).

Figure 5: Short axis stack of images using SSFP cine CMR.



Images were taken during end-diastole (top row) and end-systole (bottom row). Endocardial and epicardial contours are outlined for LV and RV from base to apex to calculate volumes and EF.

Phase-contrast velocity mapping

Using phase-contrast velocity mapping (PCVM), it is possible to determine the severity of AS via peak velocity. The velocity of flowing blood is proportional to the phase shift between stationary and moving protons in the magnetic field. Due to a lower temporal resolution, peak velocities may be underestimated when compared to echocardiography. Similar to echocardiography, misalignment between the phase direction and the flow direction can cause underestimation of velocities (28).

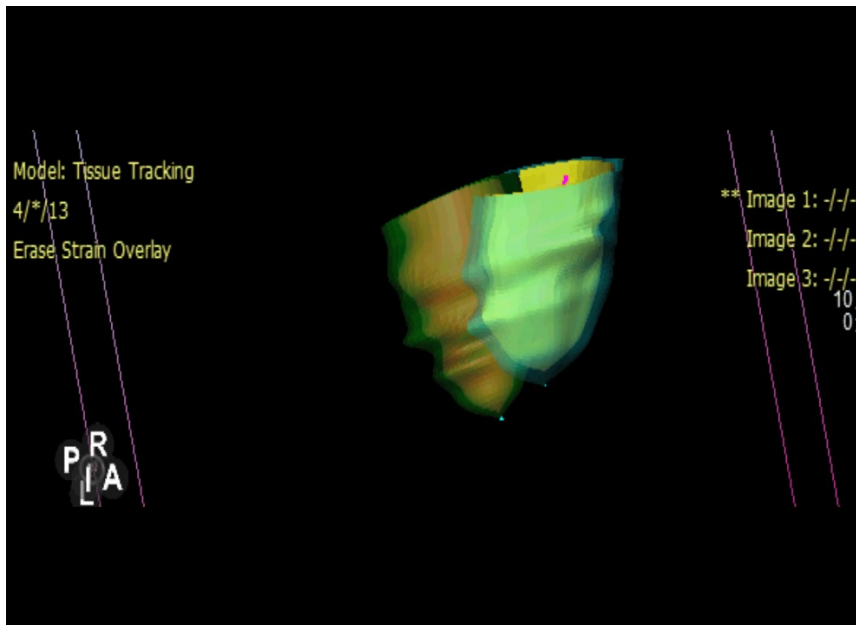
1.4.2 Post processing of CMR deformation imaging

For the analysis of myocardial deformation in CMR a technique that is most widely used today is tissue tracking. Tissue tracking is a post processing technique that can be performed on any stack of cine CMR images taken via SSFP using dedicated software. There is no need for a special sequence other than standard SSFP. Via a software algorithm anatomical features within manually or automatically defined borders are tracked

throughout the heart cycle by analysing each subsequent image and searching for the same features. These features are then tracked over time and the movement is being registered. From the resulting data parameters of myocardial deformation, such as strain or strain rate can be calculated (**Figure 4**).

By combining a stack of long- and short-axis images of the heart, the software can calculate a 3-dimensional model of the heart and its movement over one heart cycle. This movement can then be visualized as a 3D model showing differences in strain and strain-rate as a heatmap overlay. Therefore, regional anomalies in wall movement can be determined visually.

Figure 6: 3D model of the heart generated via tissue tracking.



Screenshot taken in circle cvi42® (Circle Cardiovascular Imaging Inc. Version 5.6.5, Calgary, AB, Canada).
LV and RV during end-systole.

1.5 Study aim

The aim of this study is to test the hypothesis whether RV function determined by CMR is a predictor of mortality after TAVI.

2 Methods

2.1 Study Design

We conducted a single-centre prospective study to determine the prognostic value of RV parameters obtained via CMR to test the hypothesis that pathological changes in preprocedural geometry, deformation and function of the RV predict three-year cardiovascular mortality in patients suffering from severe AS that underwent TAVI. For this purpose, we enrolled 296 patients prior to transcatheter aortic valve implantation to undergo preinterventional CMR. For the present thesis, CMR data of the cohort was analysed with a dedicated tissue tracking software (Circle Cardiovascular Imaging Inc. Version 5.6.5, Calgary, AB, Canada). The collected data included volumetric parameters as well as parameters of myocardial deformation of both the RV and LV. These data were merged with a pre-existing dataset including demographic, clinical and outcome data of the cohort, followed by statistical analysis and a comprehensive presentation of the results in this thesis.

2.2 Study Population

2.2.1 Inclusion criteria

Patients undergoing TAVI at the LKH-Universitätsklinikum Graz between May 2011 and March 2015 who received CMR prior to TAVI were included in this study. All patients presented with severe AS, defined as AVA of less than 1cm^2 as suggested in current European Society of Cardiology guidelines (14). All study participants received a CoreValve (Medtronic, Minneapolis, Minnesota) prosthesis via a transfemoral approach.

2.2.2 Exclusion criteria

Exclusion criteria were defined as unsuccessful implantation, access route different from femoral artery, different valve product and insufficient image quality in CMR as assessed visually.

2.3 Data Collection

2.3.1 Clinical data

Baseline characteristics including age, sex, Body-Mass-Index (BMI), Body Surface Area (BSA), New York Heart Association's Score for heart failure (NYHA), laboratory values

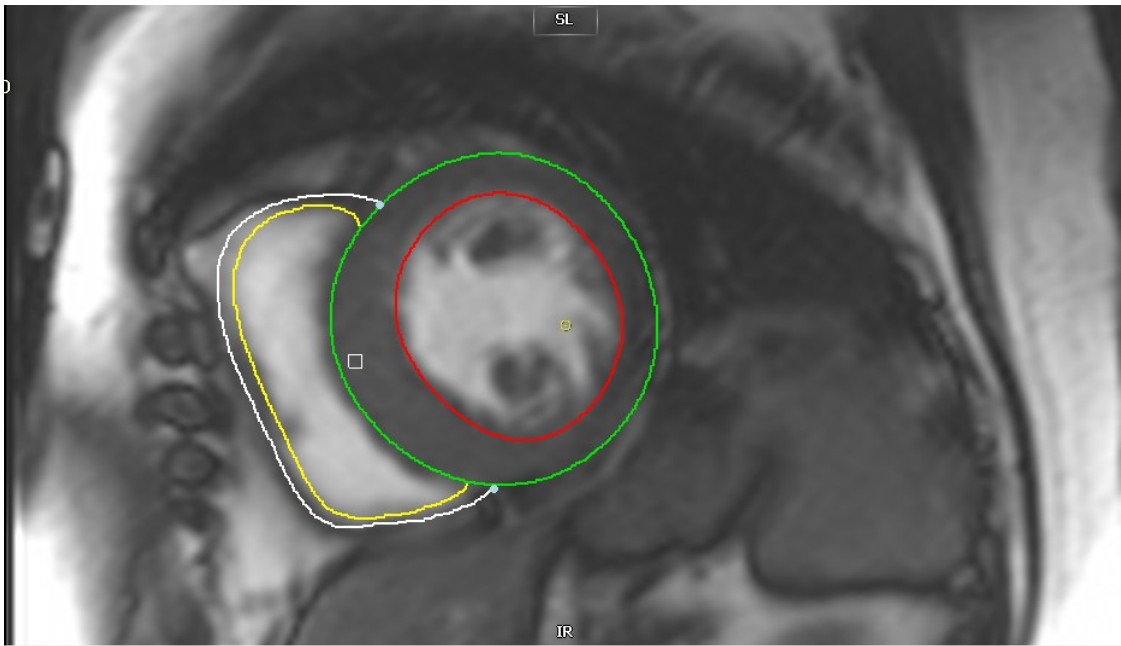
including glomerular filtration rate (GFR), N-terminal pro-B-type natriuretic peptide (NT-proBNP), troponin T high sensitive (hs-TrT), creatine kinase (CK) and creatine kinase myocardial band (CKMB) as well as echocardiographic parameters had previously been collected and were provided in a database in a pseudonymized fashion.

2.3.2 Cardiac Magnetic Resonance Imaging

2.3.3 Volumetric analysis

All CMR images acquired prior to TAVI, that had previously been pseudonymized and stored in DICOM format, were imported into cvi42® (Circle Cardiovascular Imaging Inc. Version 5.6.5, Calgary, AB, Canada) cardiovascular imaging software for analysis. To perform volumetric analysis, each patient's cine sequence was loaded in the dedicated tissue tracking module of the software. The DICOMs included cine sequences of one heart cycle in both long axis (LAX) and short axis (SAX). End-systole (ES) and end-diastole (ED) were determined manually at the points of maximal contraction and expansion of the ventricles, respectively. The valve plane was determined manually in the long axis sequence in ES and ED for both ventricles as well as the distance from valve plane to apex. Endocardium of both LV and RV was outlined manually for the complete stack of images from base to apex as recommended by the Society for Cardiovascular Magnetic Resonance (30). Papillary muscles were included in the blood volume in both systole and diastole (**Figure 7**). From the delineated volumes several parameters were calculated for both ventricles including EF, end systolic volume and EDV.

Figure 7: End-diastolic SAX slice with outlines of endo- and epicardial contours.

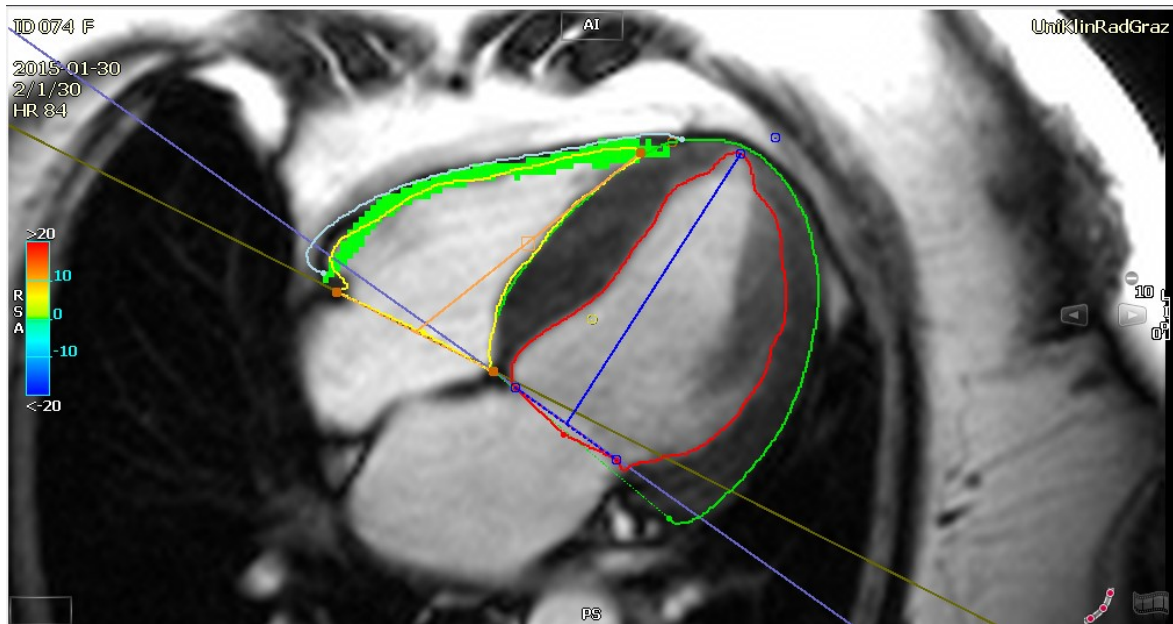


Screenshot taken in circle cvi42®. Papillary muscles included in blood volume.

2.3.4 Strain analysis

In addition to the endocardial contours, the epicardium was outlined manually in both systole and diastole within the feature-tracking module of cvi42 in ES and ED in each slice from base to apex in SAX and LAX. The most apical and most basal SAX-slices, that did not show circumferential rounded myocardium throughout the cardiac cycle, were excluded. The myocardial movement was then tracked by the software via feature tracking over the duration of one heart cycle. The operator visually checked the calculated outlines of each stack for misregistrations of the software and adjusted the contours where necessary to achieve the best representation of myocardial movement. Parameters derived from SAX were LV-GCS and RV-GCS. Parameters derived from LAX (4 chamber) were LV-GLS and RV-GLS.

Figure 8: LAX-4-chambers slice of the heart in the tissue tracking module.



Screenshot taken in circle cvi42®. Colour overlay indicating RV longitudinal strain.

2.4 Statistical Analysis

All data were saved from cvi42 into individual excel sheets (Microsoft Excel Office 365).

The target values were then combined in one Excel sheet by means of a data query. The data was merged with an existing data set containing demographic, echocardiographic, and clinical parameters as well as follow-up data including date and cause of death.

The data was imported to SPSS (Version 25, IBM, Armonk, New York, USA) for statistical analysis. All parameters were tested for normal distribution visually and by using Shapiro-Wilk test. Pearson correlation coefficient (r) was calculated between RV parameters and baseline parameters. Parameters were transformed via Box-Cox Transformation (31) to achieve normality where necessary. To assess interrater variability, 15 consecutive patients were independently analysed by a different observer. Intraclass correlation coefficient and coefficient of variation of RV-EF and RV-GLS were calculated to evaluate interobserver reliability.

Full three-year follow-up was available for all survivors. To include a maximum number of events in survival analysis, assure proportional hazards, and get the best specificity for cardiovascular events the primary endpoint was defined as cardiovascular mortality after three years. Secondary endpoints were one- and two-year cardiovascular mortality.

Cardiovascular mortality was defined according to the Valve Academic Research Consortium-2 (VARC-2) (28). Kaplan Meier Curves were plotted to illustrate survival.

Survival curves were checked visually for constant hazard ratios (HR) to fulfil criteria for Cox Regression. CMR derived parameters of LV, RV and baseline characteristics were analysed for the prediction of cardiovascular mortality after one, two and three years after TAVI via univariate cox-regression. As associations with mortality were non-proportional, follow up was truncated at the respective timepoints. Dichotomization was performed on all RV significant predictors of three-year mortality to explore possible cut-off values for practical use and to calculate HR for the individual groups. To find suitable cut-off values for dichotomization, we first performed a ROC-analysis to determine the most suitable value in terms of sensitivity and specificity for the significant predictors of three-year cardiovascular mortality via Youden-Index. If two equally suitable cut-off values arose, the one with the higher specificity was chosen. We performed univariate cox regression for the parameters that showed constant HR to test for predictive ability in terms of primary and secondary endpoints, as well as their counterparts of the contralateral ventricle for comparative reasons.

We tested for independent prediction of survival in several multivariate cox regression models including all significant RV parameters with sex, age, LV-EF, NT-proBNP, Society of thoracic surgeons risk model (STS-Score) and mean pulmonary artery pressure (MPAP).

Sample size was tested for suitability (32). For all statistical analyses, a p-value of less than 0.05 was determined to indicate significance.

3 Results

3.1 Baseline characteristics of study population

Of the 296 patients undergoing TAVI between June 2011 and February 2015, CMR was performed in 129 prior to the intervention. Two patients were excluded due to technically impossible TAVI, one due to TAVI dislocation and two with a different valve model (direct flow valve). A total of six patients were excluded for a surgical approach. Of those six, five patients were excluded due to trans-aortic access as this requires a mini-thoracotomy or mini-sternotomy, which has a different risk profile than femoral access due to its invasiveness and general anaesthesia. One patient was excluded due to trans-apical approach, which is associated with an unfavourable risk profile and possibly higher

mortality (24). A flow chart of the composition of the study population is presented in **Figure 9**.

Mean age in the elderly study population (n=112) was 81.8 years (SD=5.9), mean BMI was 26.0 kg/m² (SD=4.8) and 65% (73/112) were women. EGFR was reduced with a median of 55.3 ml/min/m² (IQR=43.3-72.8). CK and CKBM were within normal range. Median LV-EF was reduced with 53.5% (IQR=45.5-61.9, normal range for m/f = 57-77). Median RV-EF was within normal range with 56.5% (IQR=49.4-62.9, normal range f = 51-71%, m = 52-72%) and median TAPSE from CMR was 18.5 mm (IQR:13.8-23.9), also within normal range (> 16 mm). Aortic valve mean pressure gradient (AV-MPG) at 91.0 mmHg (IQR=68.9-107.6) was elevated and AVA at 0.7 cm² (IQR=0.53-0.79) was reduced, consistent with ECS definition of severe AS (12). Median pulmonary artery pressure (MPAP) at 28.0 mmHg (IQR=20.0-36.0, normal values: < 25 mmHg) (12) was elevated, consistent with pulmonary hypertension (PH). Median pulmonary capillary wedge pressure (PCWP) at 17.0 mmHg (IQR=11.5-24.0) was elevated (normal <15 mmHg). A total of 57.8% (52/90) of patients suffered from pulmonary hypertension. 9% (8/89) of patients suffered from precapillary PH compared to 48.3% (43/89) with post capillary PH (29). All cause and cardiovascular mortality after three years was 28.6% (32/112) and 21.4% (24/112) respectively. A more detailed presentation of the baseline characteristics is presented in **Table 2, Figure 10** and **Figure 11**.

Figure 9: Flow chart of study population after exclusion.

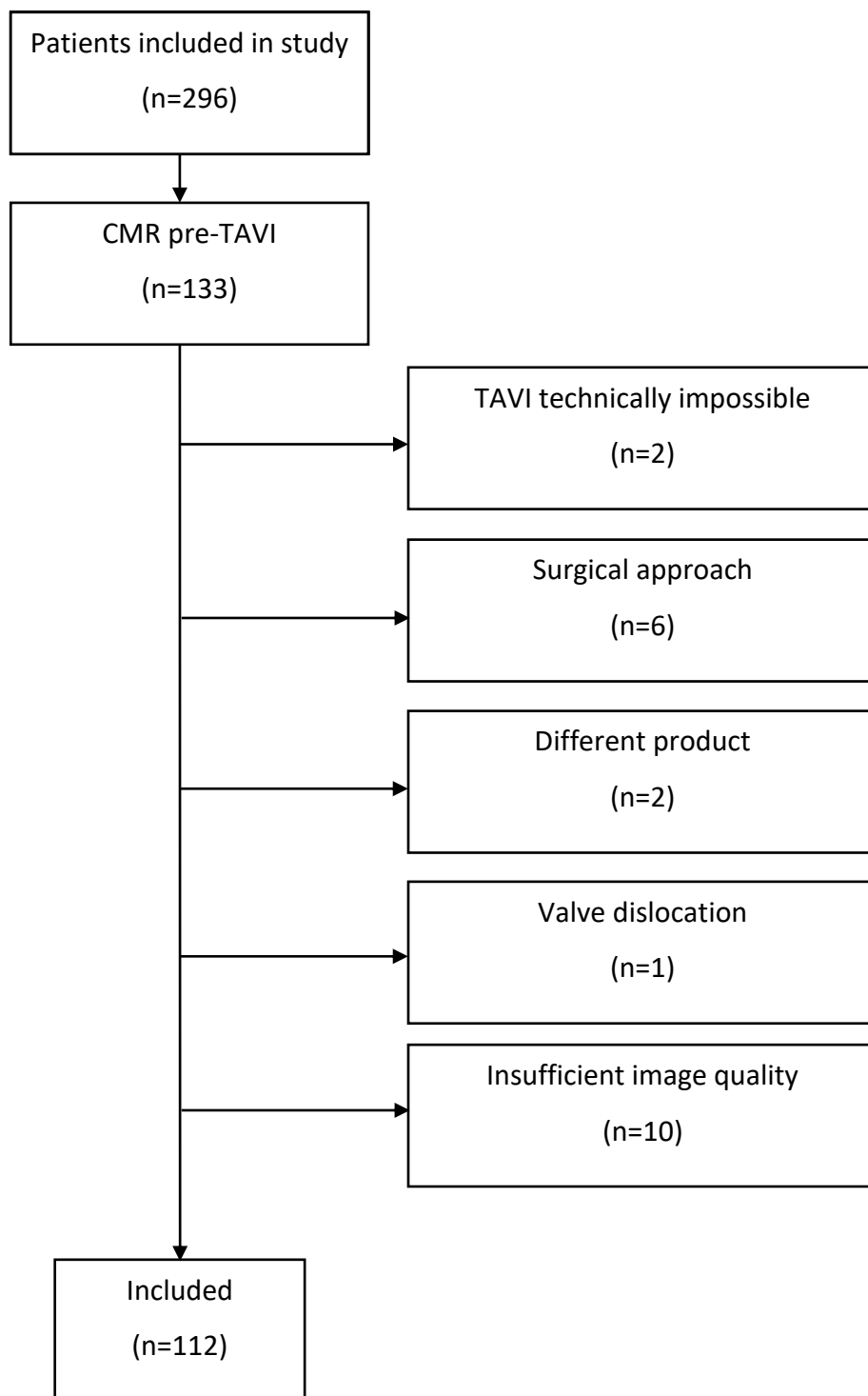
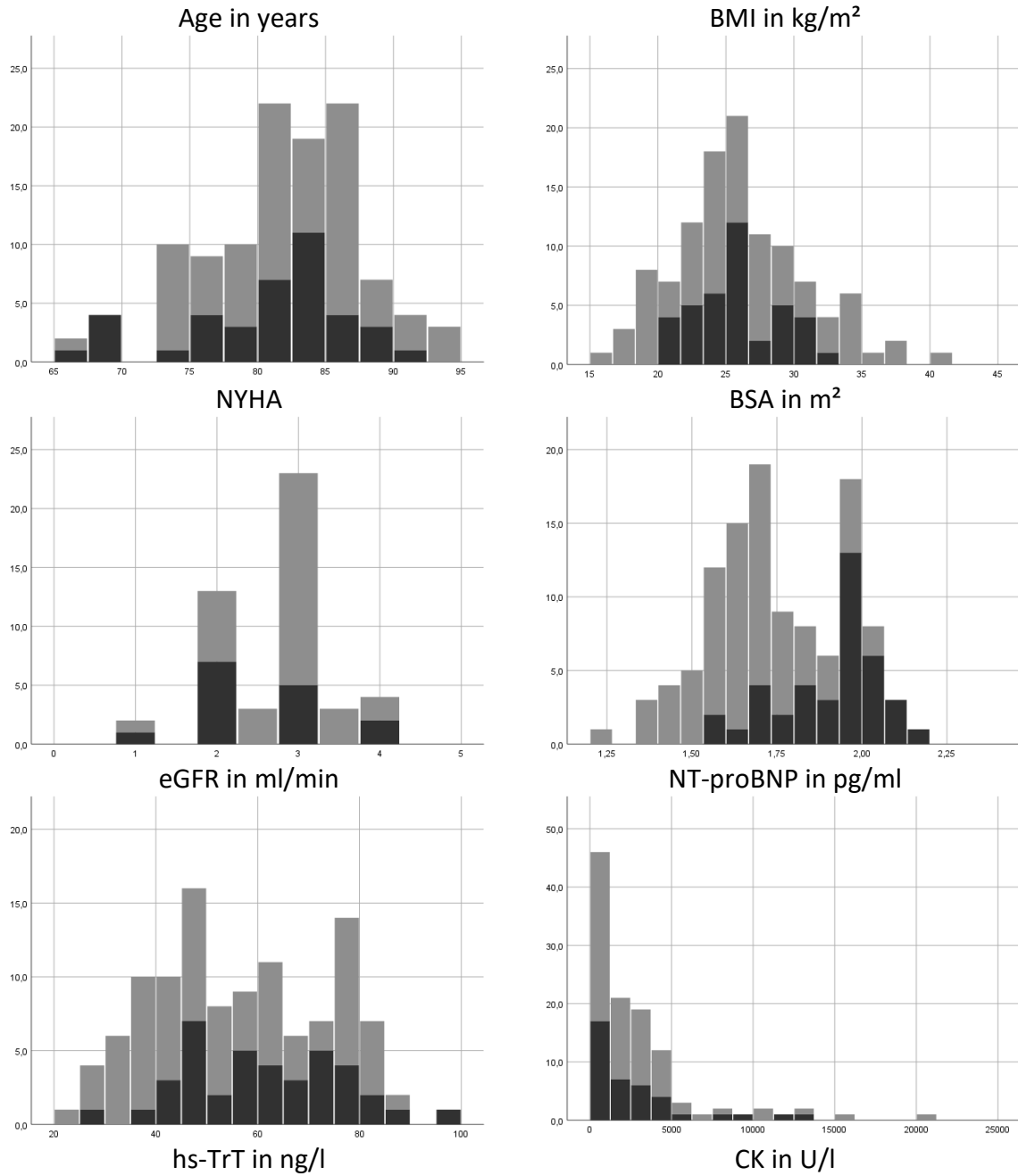


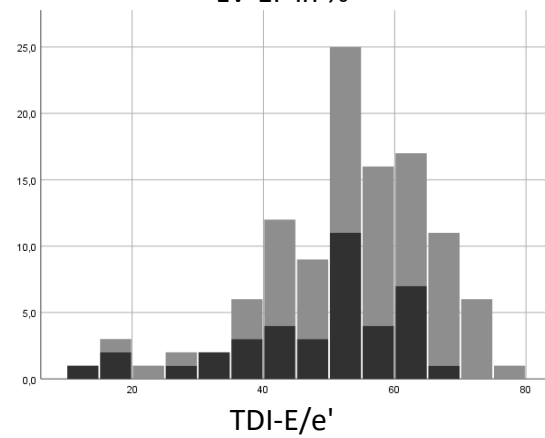
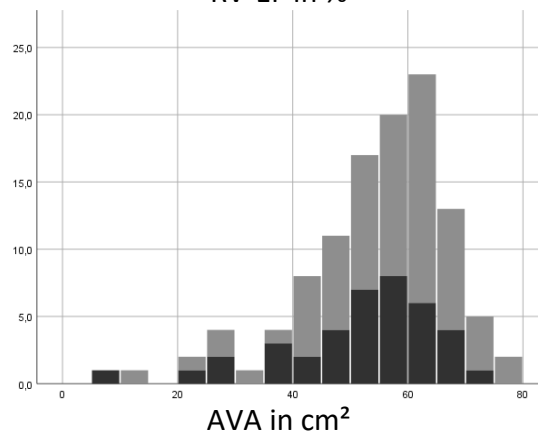
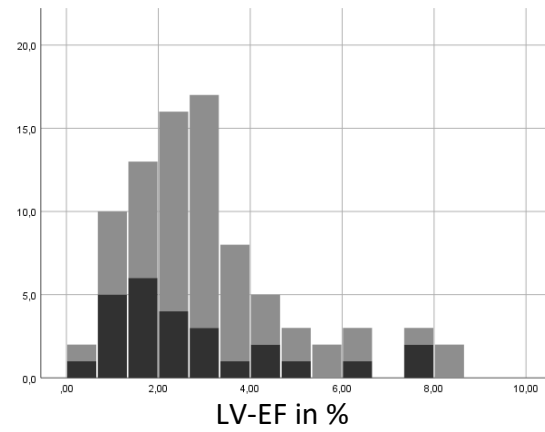
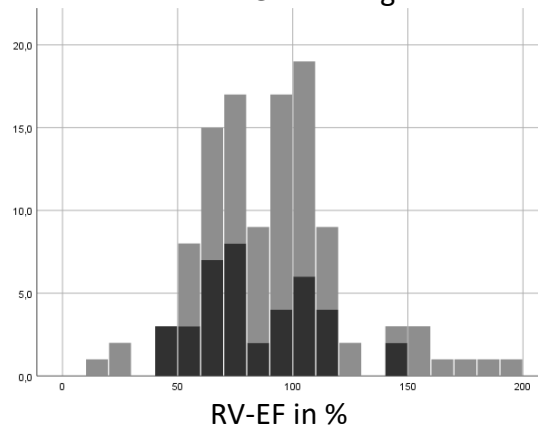
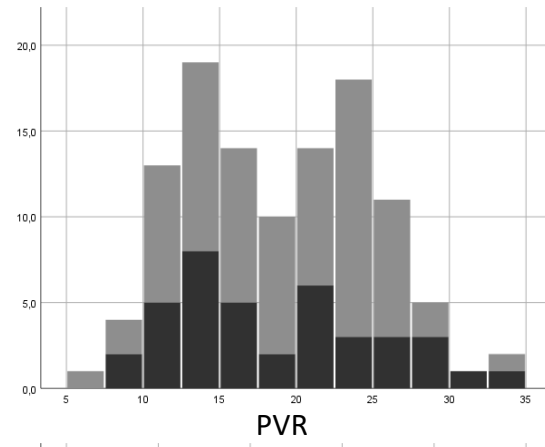
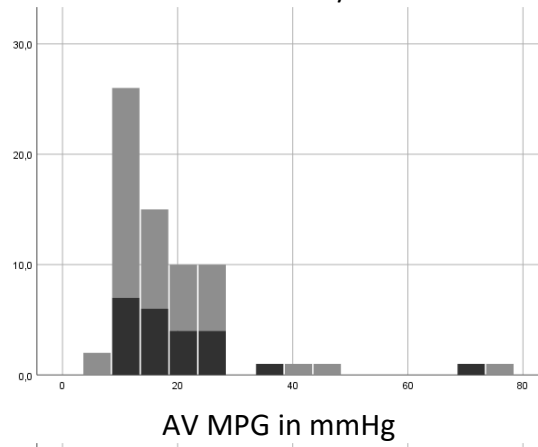
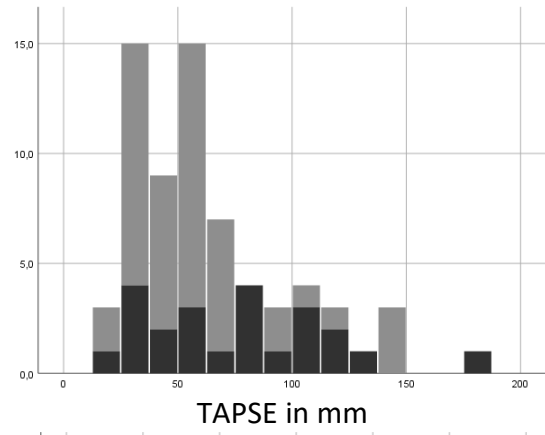
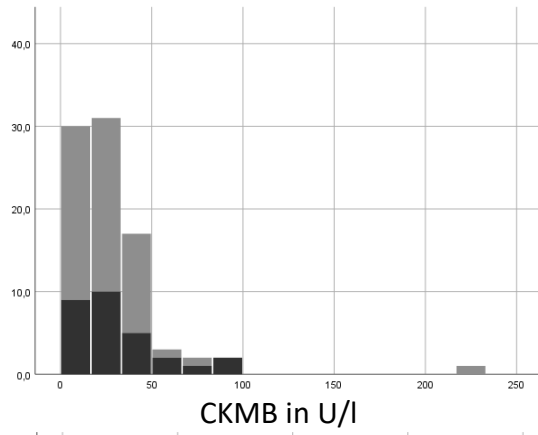
Table 2: Baseline characteristics of study population.

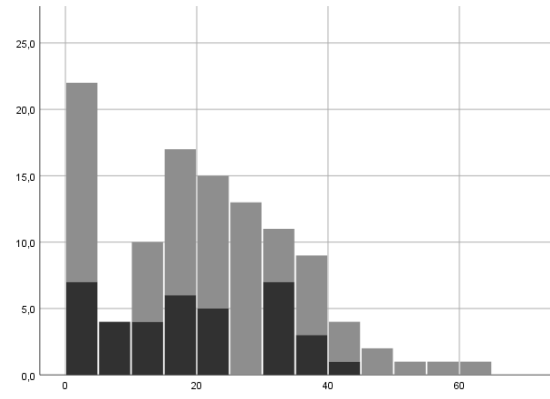
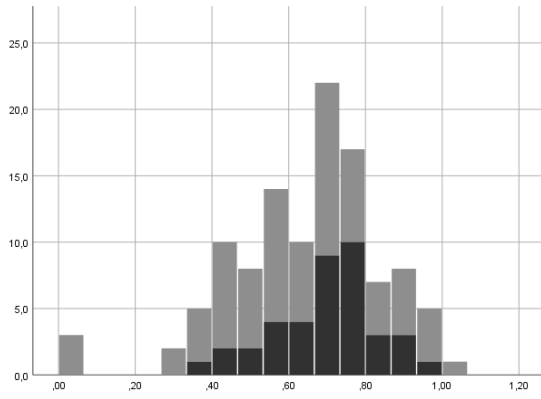
		mean/ median		SD/IQR/%	N
Demographics	Age (years)	81.8	±	5.9	112
	Female	65.2	%	(73/112)	
	BMI (kg/m²)	26.0	±	4.8	112
	NYHA	2.7	±	0.7	48
	BSA (m²)	1.8	±	0.2	112
Laboratory values	eGFR (mL/min)	55.3		[43.3-72.8]	112
	NT-proBNP (pg/mL)	1696.5		[652.5-350.3]	112
	hs-TrT (ng/l)	22.5		[12.0-38.3]	86
	CK (U/l)	57.5		[37.0-83.0]	68
	CKMB (U/l)	15.5		[11.0-21.5]	68
CMR	TAPSE (mm)	18.5		[13.8-23.9]	112
	RV-EF (%)	56.5		[49.4-62.9]	112
	LV-EF (%)	53.5		[45.5-61.9]	112
Clinical scores	EuroScoreII	4.8		[3.1-8.1]	112
	STS PROM	3.3		[2.6-5.3]	112
	AV Score	9.5		[5.6-14.6]	112
Echocardiography	AV-MPG (mmHg)	52.9		[40.8-65.7]	112
	AVA (cm²)	0.7		[0.53-0.79]	112
	TDI-E/e'	20.2		[12.2-30.4]	110
Cardiac catheter	MPAP (mmHg)	28.0		[20.0-36.0]	90
	PCWP (mmHg)	17.0		[11.5-24.0]	89
Pulmonary hypertension	pre capillary	9.0	%	(8/90)	
	post capillary	48.3	%	(41/90)	
	CPC-PH	44.0	%	(37/84)	
All-cause mortality	one year	14.3	%	(16/112)	
	two year	23.2	%	(26/112)	
	three year	28.6	%	(32/112)	
Cardiovascular mortality	one year	11.6	%	(13/112)	
	two year	17.9	%	(20/112)	
	three year	21.4	%	(24/112)	

Numbers are presented as mean ± SD, median [IQR] or percentage (n/N). N ranges between 48 and 112 due to missing data. BMI=body mass index, NYHA=New York Heart Association classification for heart failure, BSA=body surface area, eGFR=estimated glomerular filtration rate, AV-MPG=aortic valve mean pressure gradient, TDI-E/e'=tissue doppler imaging ratio between early mitral inflow velocity and mitral annular early diastolic velocity, PCWP=pulmonary capillary wedge pressure. CPC-PH combined pre- and post-capillary hypertension.

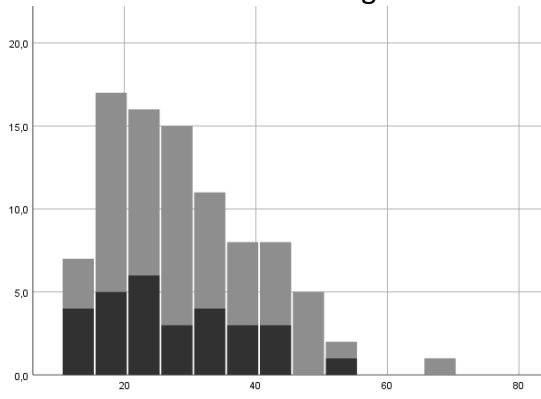
Figure 10: Histograms of baseline characteristics and standard parameters.



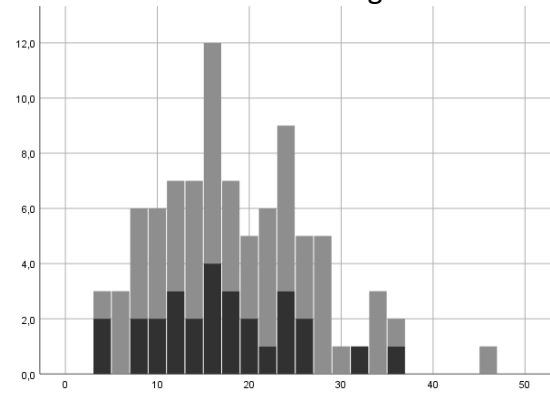




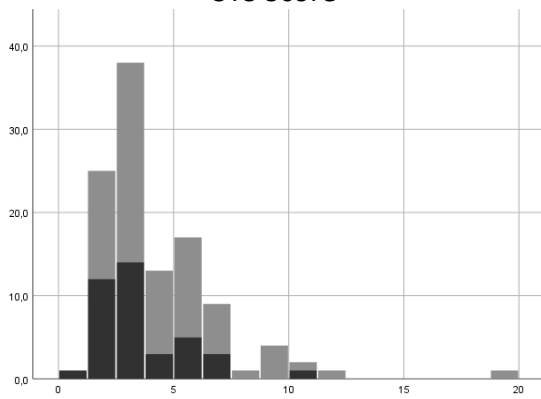
MPAP in mmHg



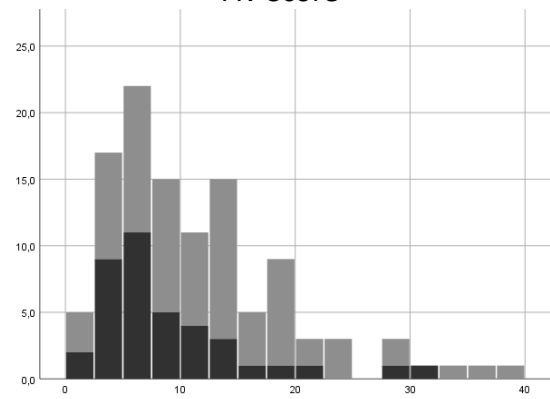
PCWP in mmHg



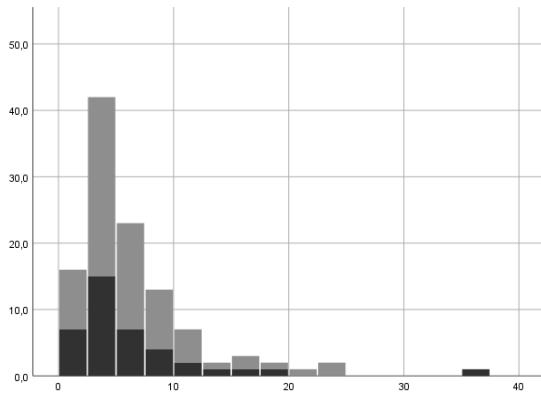
STS Score



AV Score

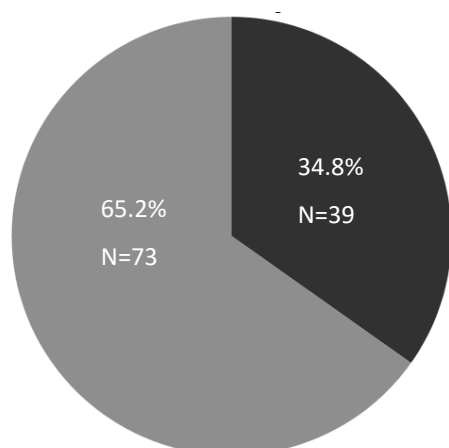


EuroScore II



Black representing male and grey colour female patients.

Figure 11: Gender distribution of patients.



Grey colour representing percentage of females (65.2% N=73) and black colour representing percentage of male patients (34.8% N=39).

3.2 Descriptive statistics of CMR parameters of volumetry and deformation imaging

Table 3: Characteristics of CMR derived parameters of volumetry and deformation.

	mean/median	(SD)/[IQR]
RV-EF (%)	56.50	[49.4-62.9]
MR-TAPSE (mm)	18.50	[64.8-90.1]
RV-EDVI (ml/m ²)	74.60	[63.2 -92.2]
RV-GCS (%)	-13.50	(-3.6)
RV-GLS (%)	-21.30	(-5.8)
RV-GRS (%)	22.90	[17.9-29.2]
LV-EF (%)	53.50	[45.5-61.9]
LV-MMI (g/m ²)	73.80	[64.8 - 90.1]
LV-EDVI (ml/m ²)	89.70	[71.0 - 106.8]
LV-GCS (%)	-17.70	[-20.9 - -14.0]
LV-GLS (%)	-13.20	(-3.9)
LV-GRS (%)	30.10	(-12.1)

N= 112 Values are mean SD or median [IQR].

3.3 Interventricular correlations of CMR parameters, Laboratory parameters and haemodynamic parameters

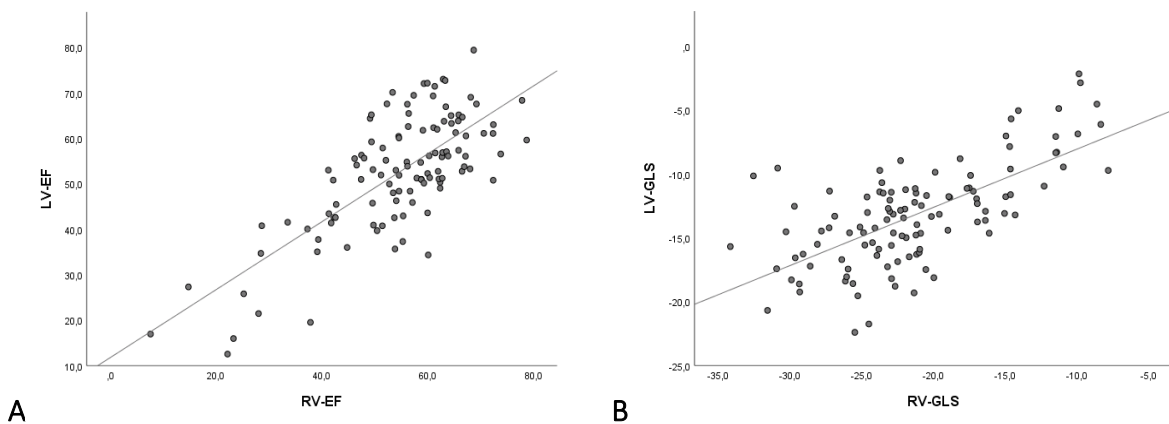
CMR derived parameters of the RV showed significant correlations with MPAP and PCWP from right heart catheter, NT-proBNP and hs-TrT from blood samples and CMR derived LV parameters. Find a detailed overview of correlations in **Table 4** and scatterplots of correlations in **Figure 12**.

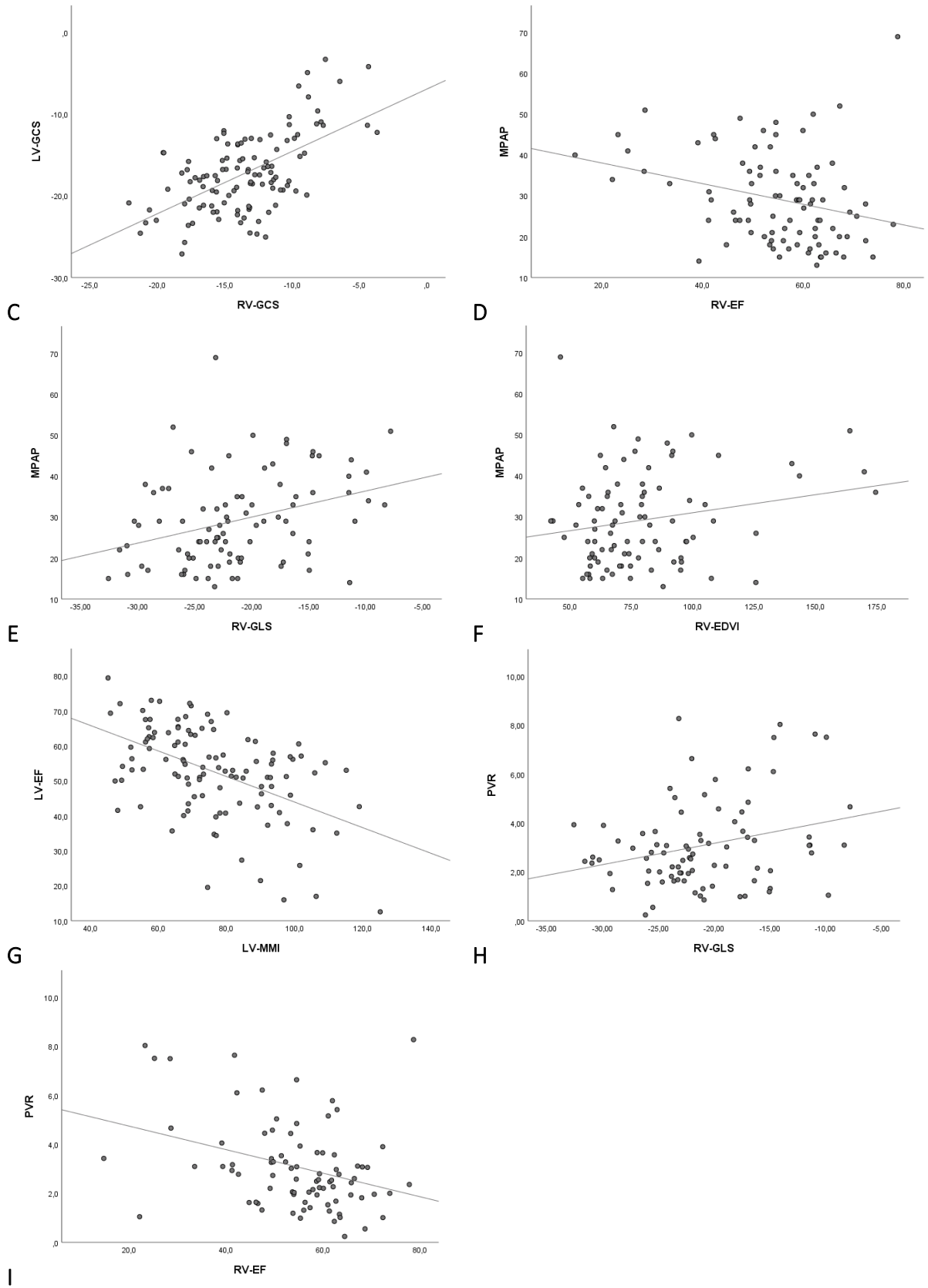
Table 4: Pearson correlations between RV parameters and pulmonary hemodynamic, LV and laboratory parameters of heart failure.

	RV-EF		RV-GCS		RV-GLS		RV-EDVI		n
	r	p	r	p	r	p	r	p	
Age	0.119	0.211	-0.082	0.391	0.062	0.518	0.136	0.154	112
MPAP	-0.159	0.135	-0.296	0.005*	0.328	0.002*	0.078	0.465	90
PCWP	0.062	0.566	0.224	0.035*	0.355	0.001*	-0.062	0.561	89
PVR	-0.336	0.002*	0.227	0.038*	0.276	0.011*	0.253	0.020*	84
LV-MMI	0.259	0.006*	0.396	0.000*	0.225	0.017*	-0.809	0.000*	112
LV-EDVI	0.385	0.000*	0.516	0.000*	0.366	0.000*	-0.967	0.000*	112
LV-EF	0.737	0.000*	-0.569	0.000*	-0.573	0.000*	0.582	0.000*	112
LV-GCS	0.517	0.000*	0.585	0.000*	0.625	0.000*	-0.533	0.000*	112
LV-GLS	0.519	0.000*	0.581	0.000*	0.672	0.000*	-0.357	0.000*	112
NTproBNP	0.405	0.000*	0.400	0.000*	0.475	0.000*	-0.389	0.000*	86
hs-TrT	-0.250	0.020*	-0.164	0.131	-0.322	0.003	0.169	0.119	86

*=p<0.05

Figure 12: Scatterplots of correlations between RV- pulmonary- and hemodynamic- parameters.





A: N=112 B: N=112 C: N=112 D: N=90 (n.s.) E: N=90 F: N=90 (n.s.) G: N=112 H: N=84 I: N=84

3.4 Survival Analysis

Median follow-up was 3.9 years (2.3-4.7). All-cause mortality after three years was 28.6% (32/112), cardiovascular mortality was 21.4% (24/112). In univariate Cox-Regression RV-EF, RV-EDVI and RV-GLS ($p=0.020$; $p=0.014$; $p=0.040$) significantly predicted three-year cardiovascular mortality. Notably none of the LV parameters significantly predicted three-year cardiovascular mortality. The presence of pulmonary hypertension (PH), whether pre- or post-capillary PH, did not predict survival. However CPC-PH, as defined in ESC guidelines (33) as a PVR of more than 3 wood units (WU) and a PCWP greater than 15 mmHg, significantly predicted cardiovascular mortality after one, two and three years ($p=0.047$, $p=0.027$, $p=0.009$). Of the clinical scores analysed, only STS score significantly predicted three-year cardiovascular mortality ($p=0.007$). The presence of peripheral artery disease (PAD) significantly predicted one- two and three-year cardiovascular mortality ($p=0.032$, $p=0.004$, $p=0.020$). See **Table 5** for a more detailed overview.

Dichotomization was performed for maximum sensitivity and specificity for three-year cardiovascular mortality both visually in ROC curves and mathematically according to Youden Index (34). The following cut-off values for CMR parameters have been determined: RV-GLS: -23.0%, RV-EF:55.5%, RV-EDVI: 78 ml/m².

After dichotomization, univariate cox regression was performed showing a HR of 2.7 (CI=1.15-6.31, $p=0.002$) in patients with RV-EF of less than 55.5%. In the group with an RV-EDVI of more than 78 ml/m² the risk of death within three years was 2.65 (CI=1.13-6.20, $p=0.025$) times increased. In the group of patients with RV-GLS of more than -23% was 2.98 (CI=1.11-7.99, $p=0.030$) times increased. The HR at two years were significantly elevated in those groups as well with HR reaching up to 4.33 (CI=1.27-14.77, $p=0.019$) for RV-GLS less negative than the cut-off value. A more detailed overview is presented in **Table 6**.

The difference in survival in the dichotomized groups is illustrated in **Figure 13**, **Figure 14** and **Figure 15** for three-year cardiovascular mortality.

In multivariate cox regression we found that RV-EF and RV-EDVI remained significant predictors for cardiovascular mortality after three years when adjusted for sex and age whereas RV-GLS remained significant when adjusted for sex (**Table 7**, **Table 8**).

We showed that RV-EF, RV-EDVI and RV-GLS in part remain significant predictors of cardiovascular mortality in Models containing STS-Score, NT-proBNP and LV-EF. For a detailed overview see **Table 9**, **Table 10** and **Table 11**.

Table 5: Univariate Cox Regression prediction of cardiovascular mortality after 1-, 2- and 3-years.

Variables	1-year		2-year		3-year	
	p	HR (95% CI)	p	HR (95% CI)	p	HR (95% CI)
RV-EF	0.081	-	0.027*	0.97 (0.94 - 01.00)	0.020*	0.97 (0.94 - 1.00)
RV-GLS	0.040*	1.10 (1.00 - 1.20)	0.035*	1.08 (1.01 - 1.16)	0.040*	1.07 (1.00 - 1.15)
RVGCS	0.433	-	0.237	-	0.209	-
RV-PSV	0.138	-	0.202	-	0.209	-
EURO Score II	0.071	-	0.138	-	0.219	-
AV Score	0.005*	1.09 (1.03 - 1.15)	0.046*	1.06 (1.01 - 1.10)	0.065	-
STS-Score	0.004*	1.21 (1.09 - 1.35)	0.011*	1.18 (1.06 - 1.31)	0.007*	1.18 (1.07 - 1.31)
RV-EDVI	0.112	-	0.018*	1.01 (1.002 - 1.018)	0.014*	1.01 (1.002 - 1.018)
LV-EF	0.935	-	0.511	-	0.406	-
LV-EDVI	0.814	-	0.143	-	0.142	-
LV-GLS	0.486	-	0.286	-	0.181	-
LV-GCS	0.754	-	0.455	-	0.352	-
Age	0.040*	1.121 (1.005 - 1.251)	0.239	-	0.122	-
MPAP	0.562	-	0.65	-	0.657	-
PCWP	0.753	-	0.518	-	0.731	-
CPC-PH	0.047*	3.853 (1.020 - 14.547)	0.027*	3.296 (1.144 - 9.499)	0.009*	3.990(1.420 - 11.209)
NYHA	0.034*	5.514 (5.514 - 26.817)	0.202	-	0.167	-
Sex	0.802	-	0.802	-	0.464	-
BMI	0.535	-	0.739	-	0.928	-
COPD	0.113	-	0.381	-	0.586	-
PAD	0.032*	3.305 (1.11 - 9.836)	0.004*	3.631 (1.503 - 8.767)	0.020*	2.588 (1.158 - 5.781)
eGFR	0.163	-	0.175	-	0.08	-
NT-proBNP	0.410	-	0.332	-	0.258	-
TnThs	0.541	-	0.291	-	0.45	-

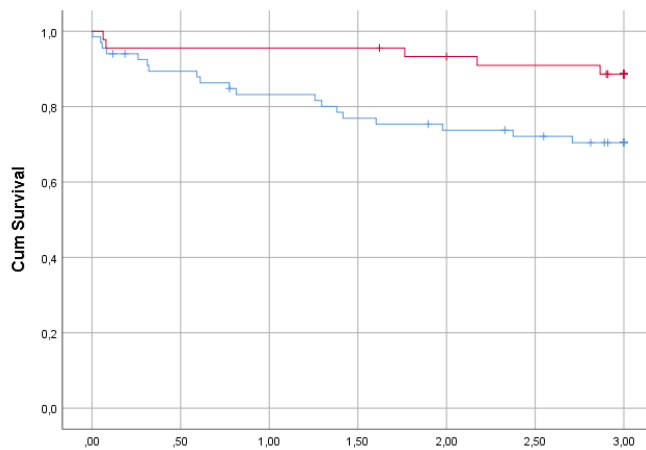
*=p<0.05.

Table 6: Univariate cox-regression for dichotomized RV-parameters for 1-, 2- and 3-year cardiovascular mortality.

variables	1 year		2 year		3 year	
	p	HR (CI 95%)	p	HR (CI 95%)	p	HR (CI 95%)
RV-EF < cut-off	0.234	-	0.022*	3.06 (1.17 - 7.97)	0.022*	2.70 (1.15 - 6.31)
RV-EDVI > cut-off	0.246	-	0.025*	3.00 (1.15 - 7.81)	0.025*	2.65 (1.13 - 6.20)
RV-GLS > cut-off	0.074	-	0.019*	4.33 (1.27 - 14.77)	0.030*	2.98 (1.11 - 7.99)

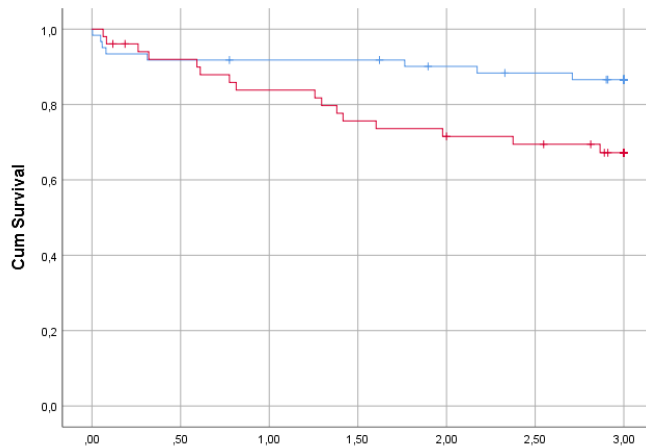
N=112, Cut-off values (Youden index): RV-GLS: -23.0%, RV-EF:55.5%, RV-EDVI: 78 ml/m². *=p<0.05.

Figure 13: Kaplan-Meier survival curve in RV-GLS groups divided by Youden Index.



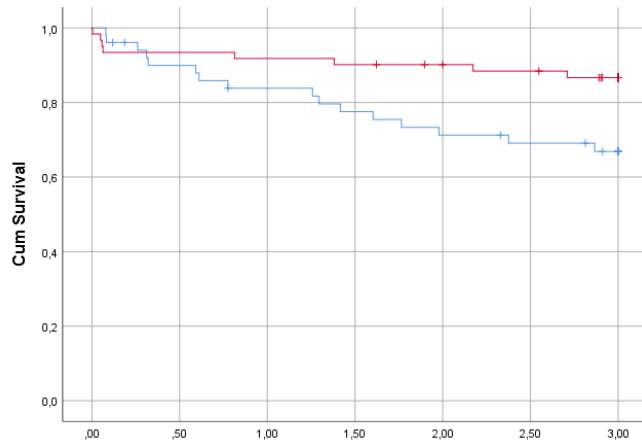
N=112. Red line: RV-GLS < -23.5%, log-rank p=0.023, x-axis=time in years.

Figure 14: Kaplan-Meier survival curve in RV-EDVI groups divided by Youden Index.



N=112. Red line: RV-EDVI > 78ml/m², log-rank p=0.019, x-axis=time in years.

Figure 15: Kaplan-Meier survival curve in RV-EF groups divided by Youden Index.



N=112. Red line: RV-EF> 56%, log-rank p=0.017, x-axis=time in years.

Table 7: RV-parameters and age in multivariate Cox regression for 3-year cardiovascular mortality.

	HR	(CI 95%)	p
Model 1			
Age	1.046	(0.973 - 1.125)	0.220
RV-EF	0.970	(0.942 - 0.999)	0.039*
Model 2			
Age	1.065	(0.988 - 1.148)	0.102
RV-EDVI	1.011	(1.003 - 1.019)	0.010*
Model 3			
Age	1.054	(0.98 - 1.133)	0.155
RV-GLS	1.068	(0.999 - 1.142)	0.052

N=112, *p <0.05.

Table 8: RV-parameters and sex in multivariate Cox regression for 3-year cardiovascular mortality.

	HR	(CI 95%)	p
Model 1			
Sex	0.811	(0.358 - 1.838)	0.616
RV-EF	0.968	(0.941 - 0.996)	0.025*
Model 2			
Sex	0.990	(0.407 - 2.407)	0.983
RV-EDVI	1.010	(1.001 - 1.019)	0.025*
Model 3			
Sex	0.874	(0.384 - 1.991)	0.748
RV-GLS	1.070	(1.000 - 1.145)	0.049*

N=112, *p <0.05.

Table 9: RV-parameters and NT-proBNP in multivariate Cox regression for 3-year cardiovascular mortality.

	HR	(CI 95%)	p
Model 1			
NT-proBNP	1.000	(1.000 - 1.000)	0.687
RV-EF	0.963	(0.928 - 0.999)	0.043*
Model 2			
NT-proBNP	1.000	(1.000 - 1.000)	0.668
RV-EDVI	1.009	(1.001 - 1.018)	0.036*
Model 3			
NT-proBNP	1.000	(1.000 - 1.000)	0.955
RV-GLS	1.071	(0.991 - 1.157)	0.082

N=112, *p <0.05.

Table 10: RV-parameters and STS-Score in multivariate Cox regression for 3-year cardiovascular mortality.

	HR	(CI 95%)	p
Model 1			
RV-EF	0.974	(0.946 - 1.003)	0.076
STS-Score	1.160	(1.041 - 1.292)	0.007*
Model 2			
RV-EDVI	1.010	(1.002 - 1.018)	0.012*
STS-Score	1.183	(1.069 - 1.311)	0.001*
Model 3			
RV-GLS	1.059	(0.991 - 1.133)	0.091
STS-Score	1.165	(1.049 - 1.293)	0.004*

N=112, *p <0.05.

Table 11: RV parameters and LV-EF in multivariate Cox regression for 3-year cardiovascular mortality.

	HR	(95.0% CI)	p
Model 1			
LV-EF	1.031	(0.985 - 1.08)	0.190
RV-EF	0.943	(0.899 - 0.989)	0.017*
Model 2			
LV-EF	1.004	(0.968 - 1.042)	0.813
RV-EDVI	1.011	(1.001 - 1.021)	0.040*
Model 3			
LV-EF	1.011	(0.971 - 1.052)	0.595
RV-GLS	1.089	(0.997 - 1.188)	0.057

N=112, *p <0.05.

3.5 Interventricular Interactions

In backwards multivariate cox regression, a model containing parameters of right-ventricular function (RV-EF, RV-EDVI, RV-GLS) and LV-EF did not produce significant improvement of model fit over RV-EF alone in prediction of cardiovascular mortality after three years in our cohort. A combination of LV-EF and left ventricular myocardial mass index (LV-MMI) to account for masked LV impairment with normal or elevated LV-EF due to LV hypertrophy in a multivariate cox regression model did not produce significant prediction of cardiovascular and all-cause mortality in neither one, two nor three-year mortality (**Table 12**).

To investigate a possible connection of RV impairment via the pulmonary circuit we ran several models in multivariate cox regression containing RV-EF, RV-EDVI, RV-GLS, MPAP and PCWP which did not produce significant prediction (**Table 13, Table 14**). In backwards cox regression models including RV-EF, EV-EDVI, RV-GLS and PCWP no combination of RV parameters and PCWP added to the prognostic value of RV-EF.

Table 12: Multivariate cox regression for cardiovascular mortality with model containing LV-EF and LV-MMI.

Variables in Model	1-year	2-year	3-year
	p	p	p
LV-EF, LV-MMI	0.996	0.510	0.530

N=112, p value of overall model.

Table 13: RV parameters and MPAP in multivariate Cox regression for 3-year cardiovascular mortality.

	HR	(CI 95%)	p
Model 1			
MPAP	0.998	(0.956 - 1.042)	0.933
RV-EF	0.972	(0.937 - 1.009)	0.134
Model 2			
MPAP	1.003	(0.964 - 1.044)	0.887
RV-EDVI	1.009	(0.994 - 1.025)	0.224
Model 3			
MPAP	1.000	(0.959 - 1.042)	0.993
RV-GLS	1.049	(0.97 - 1.136)	0.231

N=90. *p <0.05.

Table 14: RV parameters and PCWP in multivariate Cox regression for 3-year cardiovascular mortality.

	HR	(CI 95%)	p
Model 1			
RV-EF	0.973	(0.938 - 1.009)	0.136
PCWP	0.998	(0.941 - 1.058)	0.951
Model 2			
RV-EDVI	1.011	(0.996 - 1.026)	0.147
PCWP	1.003	(0.949 - 1.059)	0.924
Model 3			
RV-GLS	1.064	(0.98 - 1.156)	0.137
PCWP	0.992	(0.935 - 1.053)	0.795

N=90. *p <0.05.

3.6 Interobserver Reliability

Interrater agreement is rated excellent for RV-EF with intraclass correlation coefficient (ICC)=0.784 and good for RV-GLS with ICC=0.719 according to the guideline by Cicchetti et al. (35) Coefficient of variation (CV) was 6.06% for RV-EF and 15.43% for RV-GLS. More details are presented in **Table 15**.

Table 15: Interobserver Reliability.

Variables	ICC	95% CI	CV
RV-EF	0.784	(0.482 - 0.921)	6.06%
RV-GLS	0.719	(0.358 - 0.895)	15.43%

N=15, Comparison of independently analysed 15 consecutive patients.

4 Discussion

In this study we could confirm our hypothesis, that RV parameters predict mortality of patients with severe AS undergoing TAVI. The significant RV predictors of cardiovascular mortality were RV-EF, RV-EDVI and RV-GLS after three years.

In our analysis, RV-GCS did not significantly predict mortality. This result may be attributed to the predominantly longitudinal orientation of myocardial fibres in the right

heart as opposed to the LV. Therefore, longitudinal contraction is better reflected in RV-GLS.

Of all the analysed parameters of LV movement including LV-GLS, LV-GCS as well as several volumetric parameters, none showed significant predictive power in our cohort. Even though most clinical scores for risk assessment in patients undergoing TAVI use LV-EF among multiple factors and comorbidities, LV-EF did not predict mortality after TAVI in our cohort. This observation is consistent with recent studies describing a significant prediction of mortality by LV-EF only in the subgroup of patients suffering from low-flow, low-gradient AS (36–38).

It may seem paradox that in AS, a disease of the left heart, right heart parameters are better predictors of survival than parameters of the left heart. However, the question to ask should rather be: Which parameters can best predict disease severity and thereby prognosis? As stated earlier in the text, there are reversible and irreversible changes induced by the pathologically altered LV pressures that involve the entire cardiopulmonary system. Thus, the parameter that characterises irreversible damage most accurately, likely is the best predictor.

There are different interventricular interactions that may contribute to the fact that RV parameters appear to be more sensitive than LV parameters when it comes to predicting mortality. The best studied and most likely mechanism is via the pulmonary circulation. During the progression of AS, the increasing pressure on the LV leads to hypertrophy, fibrosis and, in the late stages, dilatation with a decrease in EF. At the same time, increasing pressure on the left atrium, sometimes in conjunction with mitral regurgitation, leads to an increase in left atrial pressure, which is reflected by the post capillary wedge pressure (PCWP). Persistently elevated PCWP over time leads to elevated pressures in the pulmonary arterial system, which in turn causes stress on the RV due to a chronically increased afterload.

We found that in our study population, mean pulmonary artery pressure MPAP and PVR were both elevated. This finding is in accordance with recent studies suggested that a form of vascular remodelling is happening in the pulmonary vascular system when confronted with chronic PH (9,11).

To pursue this approach further, we categorised those patients with CPC-PH according to the ESC guideline for pulmonary hypertension (33) using invasively measured pulmonary pressures. In univariate cox regression CPC-PH significantly predicted one-, two- and

three-year cardiovascular and all-cause mortality in our cohort with a HR reaching as high as 3.9 for three-year cardiovascular mortality.

This finding strongly supports the understanding that a pathological change in RV parameters like RV-EF, RV-EDVI and RV-GLS indicate an irreversible change, most likely in the pulmonary vascular system that prevents patients from fully recovering after TAVI.

Because the left and right hearts are highly interconnected, this may not be the only mechanism of interaction leading to RV parameters predicting mortality in AS. Other forms of interaction besides pulmonary circulation are via the septum and the common pericardium. In experimental studies, this interaction has been shown to be so strong that in *ex vivo* hearts with electrically separated ventricles pacing of only the LV produced near-normal RV pressures and output. Further research is needed to determine the extent of these connections (39).

One possible explanation for the lack of predictive ability by LV parameters, particularly LV-EF, can be explained by masking of reduced EF due to hypertrophy. Concentric geometry causes a reduction of ESV and thus tends to increase EF(40). However, neither LV-MMI alone nor a multivariate model containing LV-EF and LV-MMI did significantly predict cardiovascular survival in our cohort. A possible reason for this could be that in our study no distinction was made in the different anatomical types of hypertrophy as recommended by Duncan et al. (40). Another possible explanation might be the fact that symptoms occur well before a significant reduction of LV-EF in the vast majority of patients (38). This may have resulted in a large proportion of patients in our cohort receiving TAVI early, before a reduction in LV-EF has occurred.

LV-GLS has proven to be a reliable early marker of LV dysfunction in patients suffering from AS (33,35,37). In our cohort however, LV-GLS failed to significantly predict mortality. The reason might be a rather small sample size or the fact that the number of events was relatively small.

4.1 Limitations

The fact that this study is a single-centre study must be seen as a limiting factor for generalization. Although a sufficiently large sample of patients was reached in this study, weaker associations can be better detected in larger samples. Our cohort consisted of the

typical patient clientele presenting with high-grade AS for treatment with TAVI. Therefore, it is possible that the effects of LV parameters would be higher in a study involving more patients with low-flow low-gradient AS. The use of CMR excludes certain patient groups (pacemakers, severe renal insufficiency). This may have led to a selection bias.

4.2 Conclusion and Outlook

Right heart parameters RV-EF, RV-EDVI, and RV-GLS are predictors of intermediate term mortality after TAVI. Of these parameters, RV-GLS is of particular interest because its echocardiographic counterparts (GLS, TAPSE) can be easily and inexpensively determined. This makes RV-GLS a suitable parameter for future risk stratification in patients undergoing TAVI and might be included in clinical risk scores to improve patient selection. Furthermore, the interconnection between RV and LV via the pulmonary circuit and a possible remodelling of the pulmonary vascular system due to chronic PH might be a reason for differences in long term survival after TAVI. Further research is needed to investigate this mechanism.

5 References

1. Arsalan M, Weferling M, Hecker F, Filardo G, Kim W-K, Pollock BD, et al. TAVI risk scoring using established versus new scoring systems: role of the new STS/ACC model. *EuroIntervention J Eur Collab with Work Gr Interv Cardiol Eur Soc Cardiol*. 2018 Jan;13(13):1520–6.
2. Silaschi M, Conradi L, Seiffert M, Schnabel R, Schon G, Blankenberg S, et al. Predicting Risk in Transcatheter Aortic Valve Implantation: Comparative Analysis of EuroSCORE II and Established Risk Stratification Tools. *Thorac Cardiovasc Surg*. 2015 Sep;63(6):472–8.
3. Puri R, Iung B, Cohen DJ, Rodes-Cabau J. TAVI or No TAVI: identifying patients unlikely to benefit from transcatheter aortic valve implantation. *Eur Heart J*. 2016 Jul;37(28):2217–25.
4. Galli E, Guirette Y, Feneon D, Daudin M, Fournet M, Leguerrier A, et al. Prevalence and prognostic value of right ventricular dysfunction in severe aortic stenosis. *Eur Heart J Cardiovasc Imaging*. 2015;16(5):531–8.
5. Ren B, Spitzer E, Geleijnse ML, Zijlstra F, de Jaegere PPT, Van Mieghem NM, et al. Right ventricular systolic function in patients undergoing transcatheter aortic valve implantation: A systematic review and meta-analysis. *Int J Cardiol*. 2018 Apr;257:40–5.
6. Pschyrembel Klinisches Wörterbuch online [Internet]. [cited 2019 May 4]. Available from: <https://www.pschyrembel.de/Aortenklappenstenose/K02NK>
7. Baumgartner H, Baumgartner H, Walther T. Aortic stenosis. In Oxford, UK: Oxford University Press; Available from: <https://oxfordmedicine.com/view/10.1093/med/9780198784906.001.0001/med-9780198784906-chapter-766>
8. A. GM, S. BR, B. EC, Michael G, H. RA, T. SS, et al. Prevention of Rheumatic Fever and Diagnosis and Treatment of Acute Streptococcal Pharyngitis. *Circulation* [Internet]. 2009 Mar 24;119(11):1541–51. Available from: <https://doi.org/10.1161/CIRCULATIONAHA.109.191959>
9. Maeder MT, Weber L, Rickli H. Pulmonary hypertension in aortic valve stenosis. *Trends Cardiovasc Med* [Internet]. 2020; Available from:

- <https://www.sciencedirect.com/science/article/pii/S1050173820301584>
10. Friedberg MK. Imaging Right-Left Ventricular Interactions. *JACC Cardiovasc Imaging* [Internet]. 2018;11(5):755–71. Available from: <https://www.sciencedirect.com/science/article/pii/S1936878X18302006>
 11. Fayyaz AU, Edwards WD, Maleszewski JJ, Konik EA, DuBrock HM, Borlaug BA, et al. Global Pulmonary Vascular Remodeling in Pulmonary Hypertension Associated With Heart Failure and Preserved or Reduced Ejection Fraction. *Circulation*. 2018 Apr;137(17):1796–810.
 12. Arastéh, Keikawus, Baenkler, Hanns-Wolf, Bieber C. *Innere Medizin*. 4. Georg Thieme Verlag; 2018. online-ressource (1532).
 13. Clavel M-A, Magne J, Pibarot P. Low-gradient aortic stenosis. *Eur Heart J* [Internet]. 2016 Sep 7;37(34):2645–57. Available from: <https://doi.org/10.1093/eurheartj/ehw096>
 14. Baumgartner H, Falk V, Bax JJ, De Bonis M, Hamm C, Holm PJ, et al. 2017 ESC/EACTS Guidelines for the management of valvular heart disease. *Eur Heart J* [Internet]. 2017;38(36):2739–91. Available from: <https://doi.org/10.1093/eurheartj/ehx391>
 15. Marquis-Gravel G, Redfors B, Leon MB, Généreux P. Medical Treatment of Aortic Stenosis. *Circulation*. 2016 Nov;134(22):1766–84.
 16. Ross JJ, Braunwald E. Aortic stenosis. *Circulation*. 1968 Jul;38(1 Suppl):61–7.
 17. Joseph J, Naqvi SY, Giri J, Goldberg S. Aortic Stenosis: Pathophysiology, Diagnosis, and Therapy. *Am J Med*. 2017 Mar;130(3):253–63.
 18. Nishimura RA, Otto CM, Bonow RO, Carabello BA, Erwin JP, Fleisher LA, et al. 2017 AHA/ACC Focused Update of the 2014 AHA/ACC Guideline for the Management of Patients With Valvular Heart Disease: A Report of the American College of Cardiology/American Heart Association Task Force on Clinical Practice Guidelines. *J Am Coll Cardiol* [Internet]. 2017;70(2):252–89. Available from: <http://www.sciencedirect.com/science/article/pii/S0735109717360199>
 19. Baumgartner HC, Hung JC-C, Bermejo J, Chambers JB, Edvardsen T, Goldstein S, et al. Recommendations on the echocardiographic assessment of aortic valve stenosis: a focused update from the European Association of Cardiovascular Imaging and the American Society of Echocardiography. *Eur Heart J Cardiovasc Imaging*. 2017;18(3):254–75.
 20. Arora S, Misenheimer JA, Ramaraj R. Transcatheter Aortic Valve Replacement:

- Comprehensive Review and Present Status. *Texas Hear Inst J*. 2017 Feb;44(1):29–38.
21. Khan SU, Lone AN, Saleem MA, Kaluski E. Transcatheter vs surgical aortic-valve replacement in low- to intermediate-surgical-risk candidates: A meta-analysis and systematic review. *Clin Cardiol*. 2017 Nov;40(11):974–81.
 22. Mack MJ, Leon MB, Thourani VH, Makkar R, Kodali SK, Russo M, et al. Transcatheter aortic-valve replacement with a balloon-expandable valve in low-risk patients. *N Engl J Med*. 2019;380(18):1695–705.
 23. Biasco L, Ferrari E, Pedrazzini G, Faletra F, Moccetti T, Petracca F, et al. Access Sites for TAVI: Patient Selection Criteria, Technical Aspects, and Outcomes. *Front Cardiovasc Med* [Internet]. 2018 Jul 17;5:88. Available from: <https://pubmed.ncbi.nlm.nih.gov/30065928>
 24. Pschyrembel online [Internet]. [cited 2020 Dec 19]. Available from: <https://www.pschyrembel.de/>
 25. Abou R, van der Bijl P, Bax JJ, Delgado V. Global longitudinal strain: clinical use and prognostic implications in contemporary practice. *Heart* [Internet]. 2020 Sep 1;106(18):1438 LP – 1444. Available from: <http://heart.bmj.com/content/106/18/1438.abstract>
 26. M. SA, D. SS. Myocardial Deformation Imaging. *Circulation* [Internet]. 2012 Jan 17;125(2):e244–8. Available from: <https://doi.org/10.1161/CIRCULATIONAHA.111.086348>
 27. Seetharam K, Lerakis S. Cardiac magnetic resonance imaging: the future is bright. *F1000Research* [Internet]. 2019 Sep 13;8:F1000 Faculty Rev-1636. Available from: <https://pubmed.ncbi.nlm.nih.gov/31543951>
 28. Lopez-Mattei JC, Shah DJ. The role of cardiac magnetic resonance in valvular heart disease. *Methodist Debaquey Cardiovasc J* [Internet]. 2013;9(3):142–8. Available from: <https://pubmed.ncbi.nlm.nih.gov/24066197>
 29. Parsai C, O’Hanlon R, Prasad S. Diagnostic and prognostic value of cardiovascular magnetic resonance in non-ischaemic cardiomyopathies. *J Cardiovasc Magn Reson*. 2012 Aug 2;14:54.
 30. Schulz-Menger J, Bluemke DA, Bremerich J, Flamm SD, Fogel MA, Friedrich MG, et al. Standardized image interpretation and post processing in cardiovascular magnetic resonance: Society for Cardiovascular Magnetic Resonance (SCMR) board of trustees task force on standardized post processing. *J Cardiovasc Magn*

- Reson. 2013;15:35.
31. Box GEP, Cox DR. An Analysis of Transformations. *J R Stat Soc Ser B* [Internet]. 1964;26(2):211–52. Available from: <http://www.jstor.org/stable/2984418>
 32. Peduzzi P, Concato J, Feinstein AR, Holford TR. Importance of events per independent variable in proportional hazards regression analysis. II. Accuracy and precision of regression estimates. *J Clin Epidemiol*. 1995 Dec;48(12):1503–10.
 33. Galiè N, Humbert M, Vachiery J-L, Gibbs S, Lang I, Torbicki A, et al. 2015 ESC/ERS Guidelines for the diagnosis and treatment of pulmonary hypertension: The Joint Task Force for the Diagnosis and Treatment of Pulmonary Hypertension of the European Society of Cardiology (ESC) and the European Respiratory Society (ERS): Endor. *Eur Heart J* [Internet]. 2015 Aug 29;37(1):67–119. Available from: <https://doi.org/10.1093/eurheartj/ehv317>
 34. Kallner A. Formulas. In: Kallner ABT-LS (Second E, editor. Elsevier; 2018. p. 1–140. Available from: <https://www.sciencedirect.com/science/article/pii/B9780128143483000010>
 35. Cicchetti D V. Guidelines, criteria, and rules of thumb for evaluating normed and standardized assessment instruments in psychology. *Psychol Assess*. 1994;6(4):284–90.
 36. Povlsen JA, Rasmussen VG, Vase H, Jensen KT, Terkelsen CJ, Christiansen EH, et al. Distribution and prognostic value of left ventricular global longitudinal strain in elderly patients with symptomatic severe aortic stenosis undergoing transcatheter aortic valve replacement. *BMC Cardiovasc Disord*. 2020 Dec;20(1):506.
 37. Malkin CJ, Long WR, Baxter PD, Gale CP, Wendler O, Monaghan M, et al. Impact of left ventricular function and transaortic gradient on outcomes from transcatheter aortic valve implantation: data from the UK TAVI Registry. *EuroIntervention J Eur Collab with Work Gr Interv Cardiol Eur Soc Cardiol*. 2016 Feb;11(10):1161–9.
 38. Dahl JS, Magne J, Pellikka PA, Donal E, Marwick TH. Assessment of Subclinical Left Ventricular Dysfunction in Aortic Stenosis. *JACC Cardiovasc Imaging* [Internet]. 2019;12(1):163–71. Available from: <https://www.sciencedirect.com/science/article/pii/S1936878X18310143>
 39. Damiano RJJ, La Follette PJ, Cox JL, Lowe JE, Santamore WP. Significant left ventricular contribution to right ventricular systolic function. *Am J Physiol*. 1991 Nov;261(5 Pt 2):H1514–24.
 40. Duncan AI, Lowe BS, Garcia MJ, Xu M, Gillinov AM, Mihaljevic T, et al.

Influence of Concentric Left Ventricular Remodeling on Early Mortality After
Aortic Valve Replacement. *Ann Thorac Surg* [Internet]. 2008 Jun 1;85(6):2030–9.
Available from: <https://doi.org/10.1016/j.athoracsur.2008.02.075>